



An Updated Earthquake Catalogue and Source Model for Seismic Hazard Analysis of Pakistan

Asad ur Rahman¹ · Atif Rasheed¹ · Fawad Ahmed Najam¹ · Saeed Zaman² · Irfan Ahmad Rana¹ · Faheem Aslam¹ · Sibghat Ullah Khan³

Received: 4 October 2020 / Accepted: 3 February 2021 / Published online: 26 February 2021
© King Fahd University of Petroleum & Minerals 2021

Abstract

In this study, an updated earthquake catalogue and seismic source model for Pakistan region (bounded by latitude 20°–40° N and longitude 58°–83° E) are developed. The updated catalogue consists of published historical (10 to 1900 CE) and instrumental earthquake events (1900 to 2018 CE) with moment magnitude (M_w) ≥ 4.0 . For this purpose, several international and national databases were accessed for collecting the historical and instrumentally recorded earthquake events occurred in the study region. The collected data from various sources were homogenized in a single moment magnitude scale. Several empirical relations were developed for conversion of earthquake magnitude in other scales to moment magnitude. The datasets are homogenized, declustered, and processed to evaluate complete intervals for different magnitude ranges. Using the developed catalogue and considering the seismo-tectonic features of the region, a number of shallow and deep area source zones are delineated to develop an improved seismic source model for Pakistan. The source model for spatially smoothed background seismicity is also developed using the updated catalogue. The developed catalogue and seismic source models can be reliably used to conduct an updated probabilistic seismic hazard assessment of Pakistan.

Keywords Earthquake catalogue · Spatial smoothening · Declustering · Catalogue completeness · Seismic source model · Pakistan

1 Introduction

Pakistan lies in a seismically active and earthquake-prone region of the world. The country and its surrounding region possess a complex seismo-tectonic environment where Arabian, Indian, and Eurasian tectonic plates are interacting with different rates of movement [1]. In the northern part of Pakistan, the Indian plate is in a state of a slow head-on collision (spanning over 50–55 million years) with the Eurasian plate at a rate of 3.7–4.2 cm/year [2]. The country is located on the north-west edge of the Indian plate as shown in Fig. 1 [3]. The convergent boundary between

two continental plates, also referred to as North Collision Boundary, NCB (Fig. 1), has resulted in the development of Himalayan orogenic belt which includes some folds and thrust faults. The Himalaya Arc, Hazara Arc, Himalayan Frontal Thrust (HFT), Indus Kohistan Seismic Zone (IKSZ), and the Salt Range Thrust (SRT) are part of the NCB [1, 4–6]. The 2005 Kashmir earthquake shows a NW–SE thrust dominant mechanism, this earthquake occurred at IKSZ [7]. It has also resulted in the development of two complex subduction zones with deep brittle seismological structures; the Hindukush and the Pamir ranges [8]. In the west, the convergence of Indian and Eurasian plates forms an oblique collision zone called as West Collision Boundary (WCB) (Fig. 1). A well-known strike-slip fault (Chaman fault) and Sulaiman–Kirthar mountain ranges are the results of this inclined collision. The rate of left lateral shear between these two plates is approximately 3.0 cm/year [3]. Another complex tectonic structure, called Quetta Transverse Zone (QTZ), is located in the east of WCB as depicted in Fig. 1. The QTZ is comprised of several thrust faults (e.g. Ghazaband fault and Ornach-Nal fault) and folds that are

✉ Asad ur Rahman
asadjan1801@gmail.com

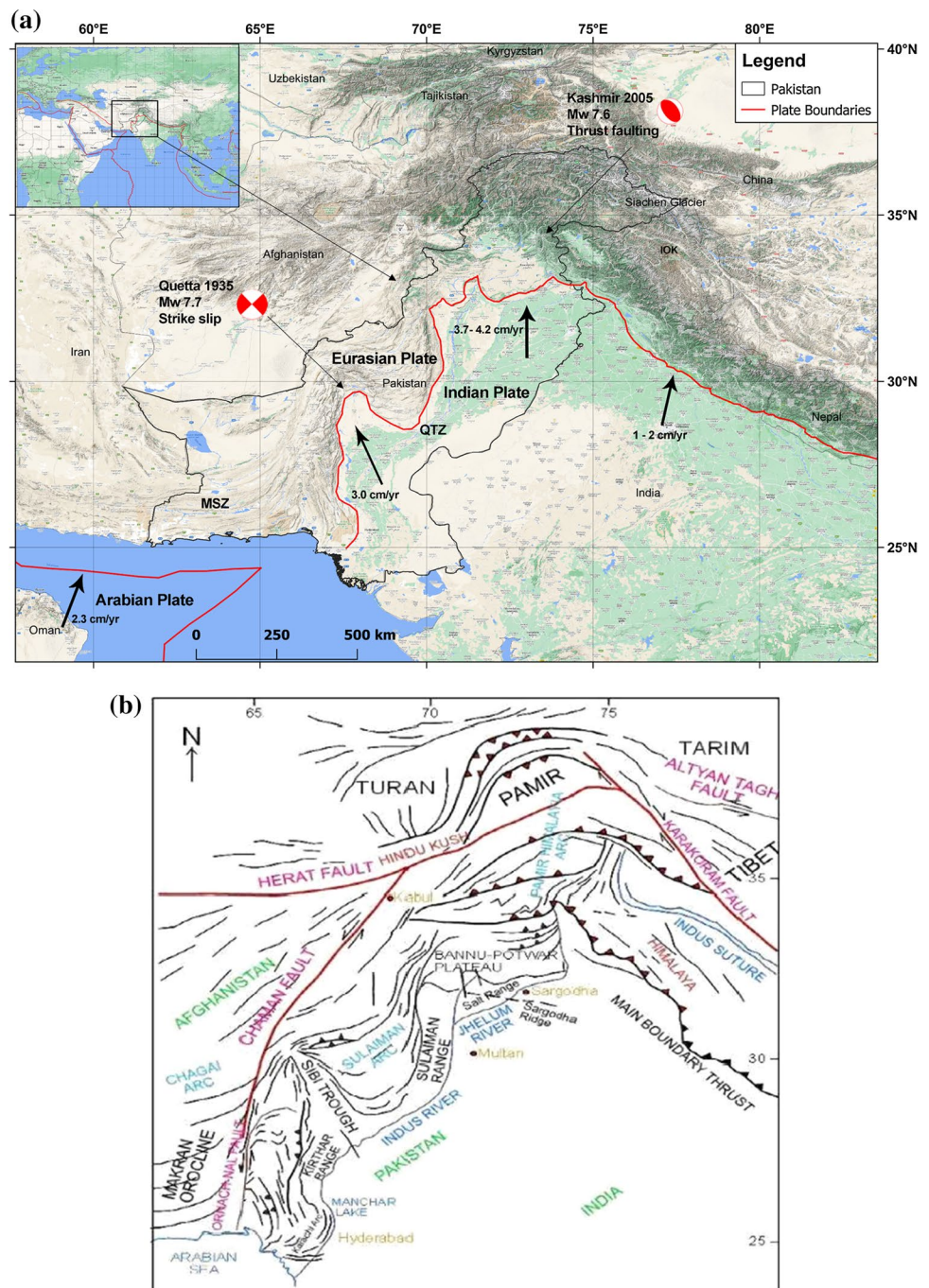
¹ National University of Sciences and Technology (NUST), Islamabad, Pakistan

² University of Engineering and Technology (UET), Jalozi Campus, Peshawar, Pakistan

³ CECOS University of IT and Emerging Sciences, Peshawar, Pakistan



Fig. 1 The tectonic setting of Pakistan. **a** shows the plate boundary between Indian, Eurasian, and Arabian Plates with their respective slip rates. **b** shows the tectonic features of the country (courtesy: Geological survey of Pakistan). The velocities of plates are extracted from Bird [64], Jade [65], Sella et al. [66], Vernant et al. [67]



associated with the Indian–Eurasian plate boundary [9]. In the south of Pakistan, the Arabian plate is subducting under the Eurasian plate at the rate of 2.8–3.3 cm/year resulting in the development of Makran Subduction Zone (MSZ) [10]. The MSZ is shown in Fig. 1 [11–13]. It is located in the south-east of Iran and southern Pakistan that extends for almost 900 km along the Eurasian–Arabian plate boundary [14]. This complex geo-tectonic environment has posed a high level of seismic hazard to Pakistan and its surrounding region.

In the last one hundred years, the country has been hit by several major earthquakes [15, 16]. These include the 2005 Kashmir earthquake ($M_w = 7.6$) and the 1945 Makran earthquake ($M_w = 8.1$) and tsunami [17]. Pakistan has severely suffered in the past from dangerous earthquakes and is still facing high seismic risk due to high seismic hazard and high vulnerabilities of communities which may lead to huge socio-economic losses in the future. With such a high level of seismic hazard and associated risk, there is a dire need for an accurate and reliable seismic

hazard assessment study of the country to develop seismic hazard maps.

In the last two decades, several studies have compiled and presented the catalogue of earthquake events for seismic hazard assessment of Pakistan [18–20]. In one of the pioneering studies, NESPAK (2007) compiled an earthquake catalogue for the probabilistic seismic hazard assessment conducted during the development of the Building Code of Pakistan [21]. This catalogue included earthquake events from 1668 to 2006 CE (see Table 1). There are several limitations attributed to this catalogue. A comprehensive set of international databases was not considered while developing this catalogue. Secondly, this catalogue includes earthquake events up to 2006. Similarly, Zare et al. [20] developed an earthquake catalogue for the Earthquake Model of Middle East (EMME) project which included the whole region of Pakistan. The earthquake events in this catalogue were reported up to 2014 CE. More recently, Khan et al. [18] have developed an earthquake catalogue which contains seismic events up to 2016 CE. To develop an updated seismic hazard map, we need our earthquake catalogue to be updated as much as possible. So, for this purpose, all of the previously compiled earthquake catalogues are combined. The recent events which were missing in the previous catalogues are included in the combined catalogue. Finally, the earthquake catalogue is critically analysed for duplicated events, dependent events, and completeness.

In this study, a relatively more updated and complete earthquake catalogue was compiled, and a seismic source model was proposed for the seismic hazard assessment studies in Pakistan. The geographical boundary was extended to 300 km from the territory of Pakistan to include all the earthquake events which may influence the hazard in the case study region. The geographical area that is bounded to longitude 20°–40° N and latitude 58°–83° E (Fig. 1) contains this composite earthquake catalogue. The earthquake catalogue was compiled using multiple earthquake catalogue sources for the period of AD 10–2018 CE. Based on this updated catalogue, a new seismic source model is also proposed. Both the conventional area source model and spatially smoothed gridded seismicity model were developed, and their recurrence parameters were reported for the seismic hazard studies in Pakistan.

2 Development of Updated Earthquake Catalogue

For data collection, the earthquake events with epicentres in Pakistan and surrounding areas, bounded by geographical limits 20°–40° N and 58°–83° E, are considered. The data of historically reported (AD 10 to 1900 CE) and instrumentally recorded (1900 CE to December 2018 CE) earthquake events are compiled using multiple international databases and local sources. The international sources include South Asian Catalogue (SACAT), International Seismological Centre [22], National Earthquake Information Centre (NEIC) [23], National Geophysical Data Centre (NGDC) [24], Global Centroid Moment Tensor (GCMT) [25, 26], and the United States Geological Survey (USGS, 2019) while the local sources include Pakistan Meteorological Department (PMD) (<http://seismic.pmd.gov.pk/>) and Water & Power Development Authority (WAPDA) (pers. comm.). The historical data were obtained from the published literature [18, 20, 27–30]. A total of 63,273 events are collected for a period of AD 10 to 2018 CE from the aforementioned earthquake databases for the region under consideration. A summary of longitude, latitude, time, depth, magnitude, and reporting agency was specified for each event in the catalogue. Table 2 shows some important data sources and the number of events reported by them for this study area.

Table 2 Earthquake databases used as sources

Period	Source	<i>N</i>	Priority order	Magnitude type
1902–2018	ISC	14,807	1	<i>mb, M_S, M_w, M_L, M_D</i>
1902–2018	USGS	12,913	2	<i>M_S, mb, M_w, M_L</i>
10–2018	NGDC	518	3	<i>M_S, M_w, mb, M_L</i>
1976–2016	GCMT	464	4	<i>M_w</i>
10–2016	[18]	7503	6	<i>M_w, M_S</i>
1965–2006	[20]	12,925	7	<i>M_w</i>
1908–2018	PMD	11,448	8	<i>M_S, M_w, mb, M_L</i>
1973–2018	WAPDA	1682	9	<i>M_w, mb, M_L</i>
1101–1964	SACAT	359	10	<i>M_S, mb, M_w, M_L</i>
25–1969	[30]	294	11	<i>mb, M_S, M_w</i>
1505–1945	[27, 29]	37	12	<i>M_S, M_w</i>
734–1994	[28]	323	13	<i>M_S, M_w</i>

N is the number of earthquakes reported by the sources, *M_S* = surface wave magnitude scale, *mb* = body-wave magnitude scale, *M_L* = local magnitude scale, *M_w* = moment magnitude scale, *M_D* = duration magnitude scale

Table 1 The earthquake catalogues compiled by different studies for the region

Study	NESPAK [19]	Khan et al. [18]	Zare et al. [20]	Current study
Time span	1668 CE–2006 CE	25 AD–2016 CE	1250 BC–2014 CE	10 AD–2018 CE
No. of events	5428	7579	7272	8108

Since earthquake data were collected from multiple sources, some events were reported by more than one source. There were duplicated events in the combined catalogue. All the duplicated events were excluded from the combined catalogue based on priority order (see Table 2) which reduced the events to 34,104. The priority order is based on the comprehensiveness of earthquake catalogues which is given in Table 2.

2.1 Magnitude Homogenization

The international databases used in this study report the earthquake events in different magnitude scales (M_w, M_S, mb, M_L , and M_D). For example, the PMD and NEIC report the events mostly in body-wave magnitude (mb), whereas the ISC database provides the events in other magnitude scales. The procedure used for the seismic hazard assessment requires the earthquake catalogue to be homogenized in terms of a single magnitude scale. For this purpose, several researchers have developed magnitude conversion equations using the regression analysis of the data which are recorded and reported in two different magnitude scales. In this study, all magnitude scales for the developed earthquake catalogue are converted to the moment magnitude (M_w) scale. Apart from using several established conversion relationships, the collected data are also used to develop new empirical equations for magnitude homogenization. These relationships are compared with those developed in a few selected studies including Khan et al. [18], Rafi et al. [31], Scordilis [32], and Zare et al. [20]. The study conducted by Scordilis [32] used the global earthquake event dataset for deriving magnitude conversion relations, while the others have used the regional earthquake datasets. The relationships developed for a particular seismo-tectonic region may result in a significant deviation from those derived for global earthquake data [33]. Therefore, in this study, new empirical relations are developed on the basis of regional dataset collected as part of developing the earthquake catalogue for the study region.

For converting body-wave magnitude (mb) to moment magnitude (M_w), an empirical relationship is developed based on the standard linear regression analysis of data shown in Fig. 2(a). Although several studies have proposed the use of nonlinear magnitude conversion relationships, e.g. Lolli et al. [34], a linear relation is developed in this study for simplicity and is presented as Eq. (1). It is developed for a total of 490 paired events having both the magnitude types (mb and M_w) collected from all the databases mentioned above. The minimum and maximum magnitude observed for those paired events are 4.0 and 6.2, respectively. Therefore, the equation is valid for the magnitude range of $4.0 \leq mb \leq 6.2$ with $R^2 = 0.7211$ and $\sigma = 0.24$.

Here, R^2 is the coefficient of determination, and σ is the standard deviation.

$$M_w = 0.967mb + 0.1989 \quad (4.0 \leq mb \leq 6.2) \quad (1)$$

Similarly, for the conversion of the surface wave magnitude scale (M_S) to moment magnitude (M_w), two linear standard regression equations are developed using the data presented in Fig. 2(b). The data are separated into two magnitude ranges (i.e. $M_S = 3.0 - 6.1$ and $M_S = 6.2 - 8.2$) since a different trend for events with $M_S > 6.2$ is observed. The bilinear regression equations (derived for this conversion) are represented in Eqs. (2) and (3). Eq. (2) is developed using 728 paired events (having both magnitude scales M_S and M_w in the catalogue) for magnitude range $3.0 \leq M_S \leq 6.1$ with correlation coefficient $R^2 = 0.69$ and standard deviation $\sigma = 0.24$, whereas Eq. (3) is derived based on 76 paired events for magnitude range $6.2 \leq M_S \leq 8.2$ with $R^2 = 0.73$ and $\sigma = 0.28$.

$$M_w = 0.5396M_S + 2.7051 \quad 3.0 \leq M_S \leq 6.1 \quad (2)$$

$$M_w = 0.9336M_S + 0.3781 \quad 6.2 \leq M_S \leq 8.2 \quad (3)$$

The relationships developed in this study are graphically compared with those developed by Khan et al. [18], Rafi et al. [31], Scordilis [32], and Zare et al. [20] in Fig. 2(c and d). Also, a tabular comparison of all selected studies is shown in Table 3.

For conversion of local magnitude (M_L) scale to moment magnitude (M_w), the common data included a total of 510 identified paired events. However, these data were scattered, and the correlation coefficient (R^2) obtained for magnitude conversion relationship was 0.20. Therefore, the empirical relationship for this conversion is not incorporated in this study. Additionally, several studies have proposed that the M_L and M_w are almost equal for magnitudes smaller than $M_w = 6.5$ [18, 20, 31, 32]. Therefore, the magnitude conversion equation by Heaton, Tajima, and Mori (1986) is employed for the conversion of local magnitude (M_L) to moment magnitude (M_w).

$$M_L = M_w \quad (M_L \leq 6) \quad (4)$$

Some of the earthquake events were reported in the duration magnitude scale (M_D) by ISC and USGS. In this current study, the duration magnitude was converted to M_w by using the relationship developed by Akkar et al. [35] as presented in Eq. (5) as follows.

$$M_w = 0.764M_D + 1.379 \quad 3.7 < M_D < 6.0 \quad (5)$$



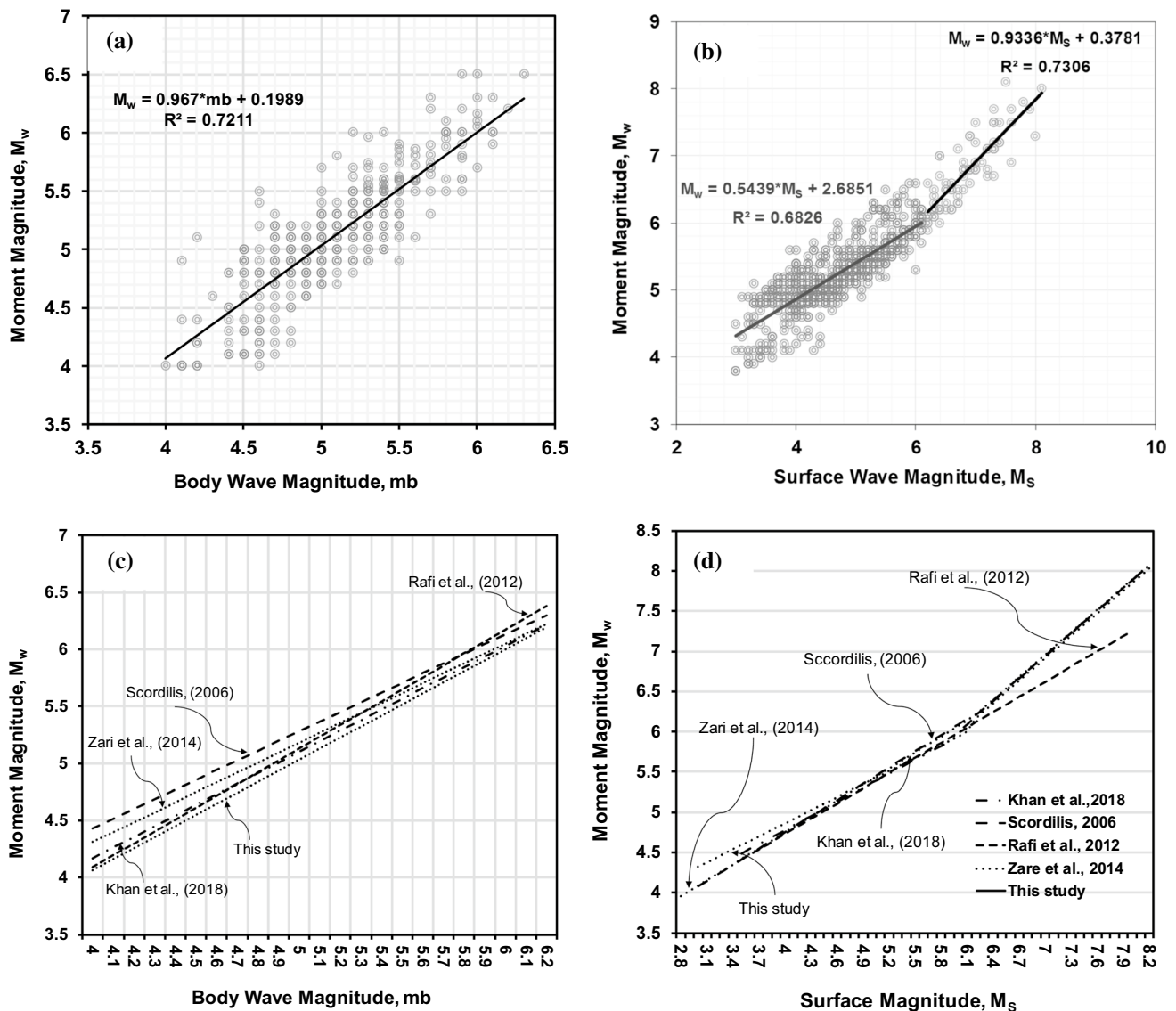


Fig. 2 a and b show the relationships developed for converting mb and M_S to M_w , using data from all the databases mentioned above. c and d show a comparison of the magnitude conversion relationships with the previous studies

Finally, a priority order for earthquake events based on the magnitude scale was set to collect the data. The priority order for $M_w, mb, M_S, M_L,$ and M_D is set as 1, 2, 3, 4, and 5, respectively. After the homogenization of earthquake events, the catalogue had a total of 63,273 events. The identification of same/duplicated events (reported by different constituent catalogues) was performed after homogenizing the magnitude. The events having identical year, month, day, hour, minute and having almost the same coordinates are considered as same/duplicated events. All the duplicated events were manually excluded from the combined catalogue, based on priority order as shown in

Table 2. This process reduced the total number of events to 34,104.

2.2 Declustering of Earthquake Events

One of the basic assumptions of the probabilistic seismic hazard assessment (PSHA) is that the earthquake events are statistically independent and occur randomly in time. Such process is mathematically described as a Poissonian stochastic process or a process having Poissonian distribution. Based on this assumption, several methodologies have been proposed to identify the dependent events in a time–space window around the mainshock event. The removal of such

Table 3 Comparison of magnitude conversion relations

Magnitude type	Homogenization relation	Magnitude range	R^2	N	σ	Reference
mb, M_w	$M_w = 0.967mb + 0.198$	$4.0 \leq mb \leq 6.2$	0.7211	459	0.24	This study
	$M_w = 0.93mb + 0.45$	$4.0 \leq mb \leq 6.2$	0.71	286	0.18	[18]
	$M_w = 0.87mb + 0.83$	$3.5 \leq mb \leq 6.0$	0.88	16,752	0.3	[20]
	$M_w = 0.85mb + 1.03$	$3.5 \leq mb \leq 6.2$	0.57	3978	0.29	[32]
	$M_w = 1.04mb - 0.07$	$4.0 \leq mb \leq 6.9$	0.72	4		[31]
M_S, M_w	$M_w = 0.53M_S + 2.70$	$3.0 \leq M_S \leq 6.1$	0.6973	728	0.25	This study
	$M_w = 0.93M_S + 0.37$	$6.2 \leq M_S \leq 8.2$	0.7306	76	0.28	
	$M_w = 0.58M_S + 2.46$	$3.5 \leq M_S < 6.0$	0.75	597	0.07	[18]
	$M_w = 0.94M_S + 0.36$	$6.0 \leq M_S \leq 8.2$	0.91	165	0.15	
	$M_w = 0.66M_S + 2.11$	$2.8 \leq M_S \leq 6.1$	0.94	4123	0.28	[20]
	$M_w = 0.93M_S + 0.45$	$6.2 \leq M_S \leq 8.2$	0.88	129		
	$M_w = 0.67M_S + 2.07$	$3.0 \leq M_S \leq 6.1$	0.77	23,921	0.17	[32]
	$M_w = 0.99M_S + 0.08$	$6.2 \leq M_S \leq 8.2$	0.81	2382	0.2	
	$M_w = 0.63M_S + 2.21$	$3.5 \leq M_S \leq 8.0$	0.84			[31]

dependent events from the earthquake catalogue results in a Poissonian distribution of seismicity in a region. This process in which the earthquake events (mainshocks) are segregated from the dependent events is called declustering [36]. For this purpose, four studies including Gardner, Knopoff [36], Reasenberg [37], Uhrhammer [38], and Gruenthal (Zare et al. [20]) are selected in this study. These studies propose different methods for declustering the earthquake catalogue. They are selected after the review of available literature. More importantly, their algorithms and source codes were also easily available.

The results obtained from these methods generally suggest different sizes of the time and space windows for declustering. The size of the time and space window is directly proportional to the magnitude of the mainshock. The collection of earthquake events that occur in that time and space window is called a seismic cluster. The earthquake event with a higher magnitude in the seismic cluster is considered as the mainshock, whereas the events within that spatial window of space and time frame with reference to the mainshock are regarded as dependent events [37]. The values suggested by Reasenberg [37] algorithm for the default standard parameter are represented in Table 4. Foreshocks and aftershocks are the dependent events that occur before and after the mainshock, respectively. Therefore, the foreshocks and aftershocks are required to be eliminated from the catalogue as these events are considered to be dependent events over the mainshock.

Table 5 shows the empirical relationships for determining the size of time and space window proposed by Gardner, Knopoff [36], Uhrhammer [38], and Gruenthal (Zare et al. [20]). The catalogue developed in this current study was declustered separately by employing these four algorithms using the ZMAP software package [39]. The total number of clusters and remaining events after the application of each

Table 4 Declustering input parameters recommended by Reasenberg [37]

Parameter	Standard	Simulation range	
		Min	Max
τ_{min} [days]	1	0.5	2.5
τ_{max} [days]	10	3	15
P	0.95	0.9	0.99
x_{meff}	4.0	0	1
x_k	0.5	1.6	1.8
r_{fact}	10	5	20

Here, τ_{min} is the minimum value of the look-ahead time for building clusters when the first event is not clustered, τ_{max} is the maximum value of the look-ahead time for building clusters, P is the probability of detecting the next clustered event used to compute the look-ahead time, τ ; x_k is the increase in the lower cutoff magnitude during clusters: $x_{meff} = x_{meff} + x_k M$, where M is the magnitude of the largest event in the cluster, x_{meff} is the effective lower magnitude cutoff for catalogue, r_{fact} is the number of crack radii surrounding each earthquake within new events considered to be part of the cluster [68]

method of declustering is shown in Table 6. In this study, the catalogue obtained after the declustering method proposed by Gardner, Knopoff [36] is used for determining the seismic hazard parameters. Several similar studies focussed on the hazard analysis of this region including Zare et al. [20] and Khan et al. [18] have also preferred the use of declustering method developed by Gardner, Knopoff [36]. The spatial distribution of final declustered earthquake events is presented in Fig. 3.

2.3 Data Completeness

Incompleteness in the catalogue is the difference in recorded and real seismicity of the region [40]. Catalogue incompleteness is considered as an important uncertainty of an

Table 5 The windows size approximation by Gardner and Knopoff (1974), Uhrhammer (1986), and Gruenthal (Zare et al. [20])

Method	Distance (km)	Time (days)
Gardner and Knopoff [36]	$10^{0.1238 M+0.983}$	$10^{0.032M+2.7389}$ if $M \geq 6.5$ $10^{0.5409M-0.547}$, else
Uhrhammer [38]	$e^{-1.024+0.804 M}$	$e^{-2.87+1.235 M}$
Gruenthal (Zare et al. [20])	$10^{1.77+(0.037+1.02M)^2}$	$e^{-3.95+(0.062+17.32M)^2}$ if $M \geq 6.5$ $10^{2.8+0.024M}$, else

Table 6 Number of events after declustering

Method	Total events	Number of clusters	Number of events remained	Number of events removed (%)
Gardner, Knopoff [36]	34,104	3454	7845	26,259 (76.93%)
Reasenber [37]		4387	26,495	11,976 (35.12%)
Uhrhammer [38]		4629	15,706	18,378 (46.05%)
Gruenthal		2688	4929	29,175 (85.54%)

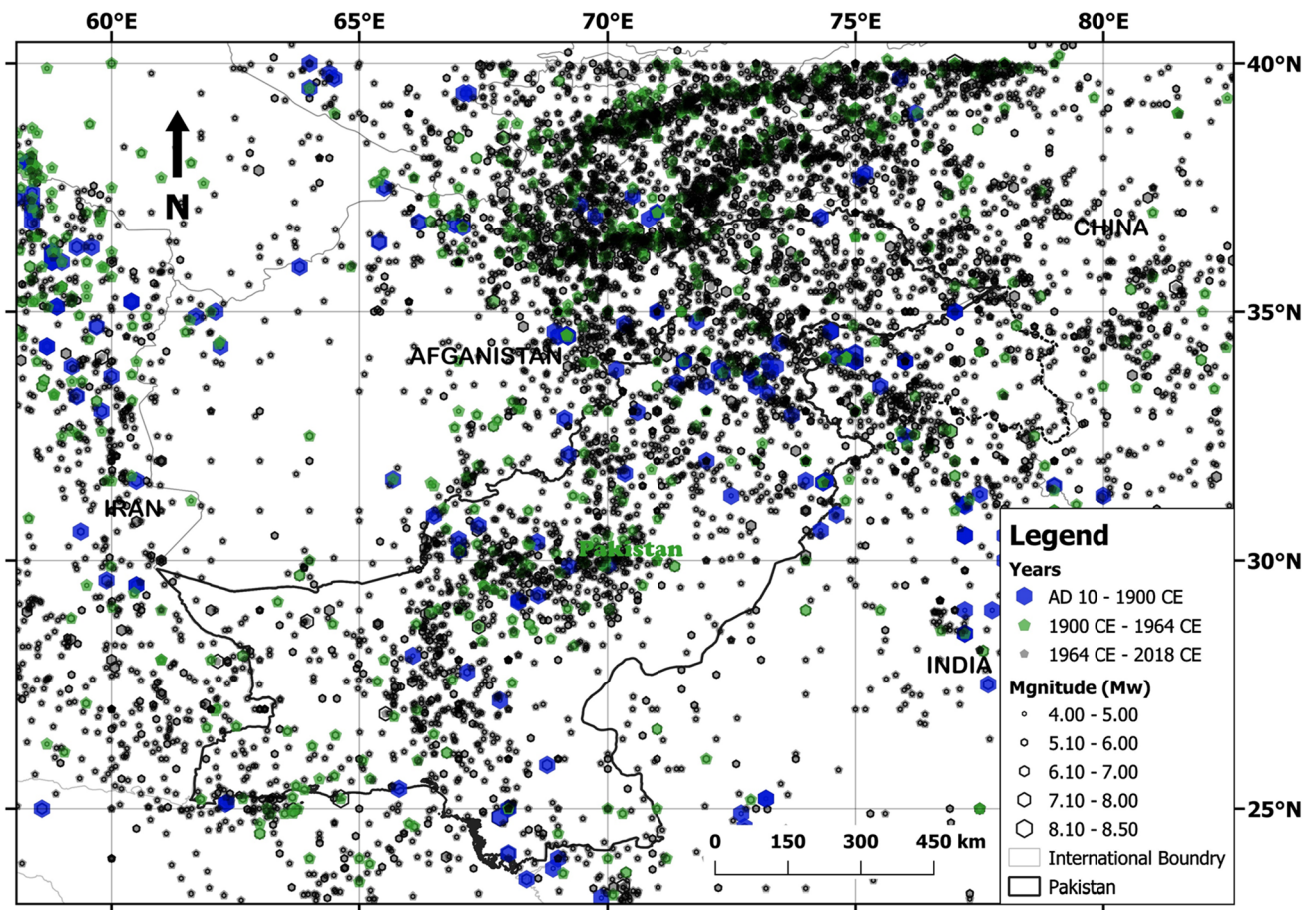


Fig. 3 Temporal and spatial distribution of final declustered earthquake catalogue consisting of 7845 earthquake events

earthquake catalogue in seismic hazard analysis. The earthquake catalogue must be complete to be used in any seismic hazard assessment study. Since in the past the earthquake recording instruments were insufficient to record every possible earthquake event. Therefore, the available data of past earthquakes are very scarce. This scenario brings forward the uncertainty of completeness in catalogue. The temporal distribution of earthquake events from 10 to 2018 CE is shown in Fig. 4.

There are several methods to measure the completeness of the catalogue with respect to magnitude and time. In this study, two techniques; Visual Cumulative Method (CUVI) [41] and Stepp [42] method; are employed. The CUVI method [41] is a simple graphical procedure. It is based on the visual observation in which complete earthquakes of a given magnitude are assumed to follow a stationary occurrence process (straight line). Furthermore, the declustered catalogue is divided into nine magnitude classes. The magnitude classes are incremented with a 0.5 magnitude bin, i.e. 4 – 4.5 and 4.5 – 5, etc. (Table 7). For every magnitude class, a graph is constructed between the cumulative number of events and the time period in years. So, for each magnitude class, the period of completeness is the approximate straight line starting from the point where the trend gets stabilized. The initial point is called magnitude of completeness (M_C). Similarly, Woessner, Wiemer [43] defined magnitude of completeness, M_C , as the lowest recorded magnitude at which approximately all the events are detected. It is also known as threshold magnitude. The magnitude of completeness (M_C) has an important role in the calculation of seismicity parameters (' a ' and ' b ' values) for seismic sources using Gutenberg, Richter [44] relationship. In this current study, the magnitude frequency distribution (MFD) by Gutenberg, Richter [44] is used for calculating

Table 7 Completeness ranges for every magnitude class

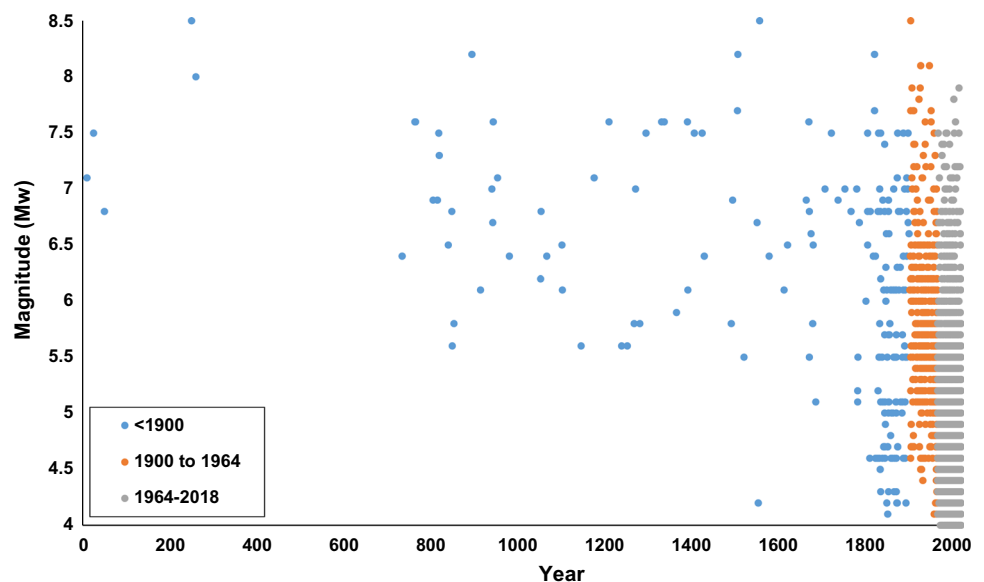
Magnitude class	Completeness period
$M_w \geq 4.0$	1990–2018 = 28
$M_w \geq 4.5$	1975–2018 = 43
$M_w \geq 5.0$	1951–2018 = 67
$M_w \geq 5.5$	1926–2018 = 92
$M_w \geq 6.0$	1900–2018 = 118
$M_w \geq 6.5$	1900–2018 = 118
$M_w \geq 7.0$	1900–2018 = 118
$M_w \geq 7.5$	1884–2018 = 134
$M_w \geq 8.0$	1878–2018 = 140

the magnitude of completeness (M_C) within each seismic source. A graph between the magnitudes and logarithm of the cumulative number of events is drawn. The maximum curvature of the graph gives the magnitude of completeness for each set of events, as shown in Tables 9 and 10. The method is applied using the ZMAP software package [39].

The Stepp [42] method is based on the mean rate of recurrence of earthquakes (λ) in a given time and magnitude class, this method classifies the earthquake catalogue on the basis of magnitude and time (years) intervals as represented in Eq. 6. For the completeness analysis applying the Stepp [42] method, the OpenQuake engine [45] is used.

In this study, both the methods were employed and the results from both methods (CUVI and Stepp (1973)) yielded similar completeness periods. The completeness periods for different magnitude classes are shown in Table 7. It is a common observation that larger magnitude earthquakes are rarely missed as compared to the smaller magnitude events in history. This is the reason that the completeness range of larger magnitudes is higher as compared to the smaller

Fig. 4 Plot showing the temporal distribution of events for Pakistan and surrounding areas bounded by geographical limits 20°–40° N and 58°–83° E. Events are plotted from 10 to 2018 CE



magnitudes, which are complete only within the instrumental period.

2.4 Seismogenic and Focal Depths

The maximum observed depth in any seismogenic zone at which most of the earthquakes occur is called seismogenic depth (D_{seis}) [46]. In geophysics, the seismogenic layer includes all the depths of earthquakes which mostly occur in the lithosphere or crust of the earth [47]. To get a better insight into the tectonics of the region and to determine the seismic hazard, the accurate determination of the focal depths of earthquakes is extremely important [48]. For this reason, the final catalogue was mapped, and Fig. 5 represents the earthquakes based on focal depths. Based on focal depths, the seismic area sources are classified into shallow and deep seismic sources. Figure 5 is depicting that the seismicity of Pakistan is spread all over the country. However, deeper earthquakes are focussed in the northern areas of Pakistan.

The depth of seismogenic layers is related to the size of earthquakes which are generated by active faults. This is the

reason that it's a significant parameter for the assessment of seismic hazard [49]. Some intermediate-depth events at about 70° E 24° N where only shallow seismicity seems to occur shows a pattern are actually the area of Kachchh mainland fault and Nigarparkar fault (Fig. 5). Another important pattern of earthquakes at an area approximately 65°–68° E 25°–28° N shows shallow seismicity with some intermediate-depth events is the area of Chamman, Ghazaband, and Ornachnal-Nal faults. Similarly, the deeper seismicity of Hindukush region can be seen in the northern areas of Pakistan and Afghanistan (Fig. 5).

Therefore, the ultimate declustered catalogue (Fig. 3) is further divided into shallow- (depth < 50 km) and intermediate-depth earthquakes (depth < 50 km) as shown in Figs. 6 and 7, respectively. The data in these figures are displaying that most of the seismicity of Pakistan is due to shallow earthquakes. Shallow earthquakes contribute 83%, while the deep earthquakes have only a 17% contribution. Most of the deeper earthquakes are located in the northern part of Pakistan and around the plate boundary, while some intermediate-depth earthquakes are also observed in the south-western part of the country. The research carried out by the Pakistan Meteorological

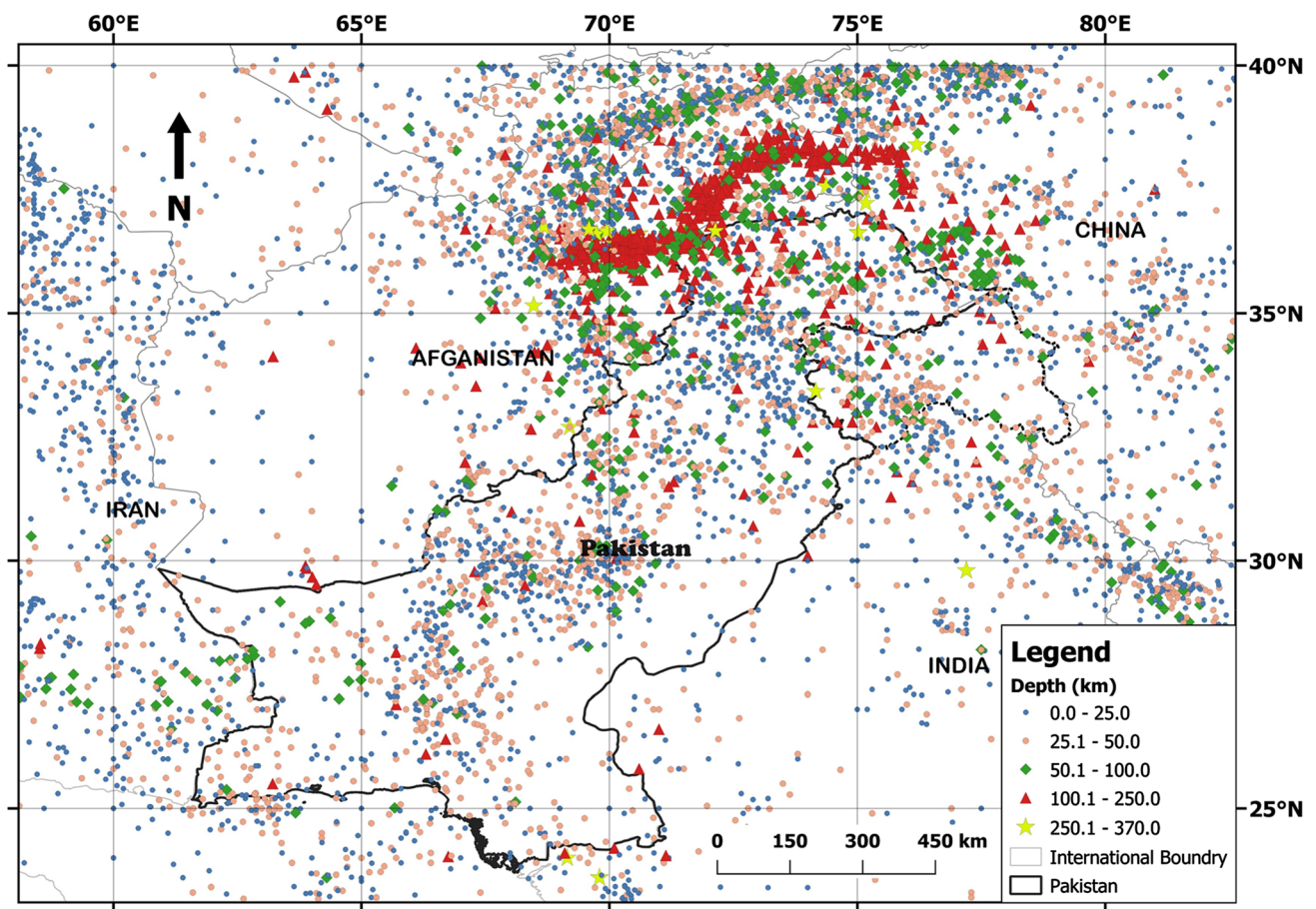


Fig. 5 Earthquake events in the catalogue with different focal depths

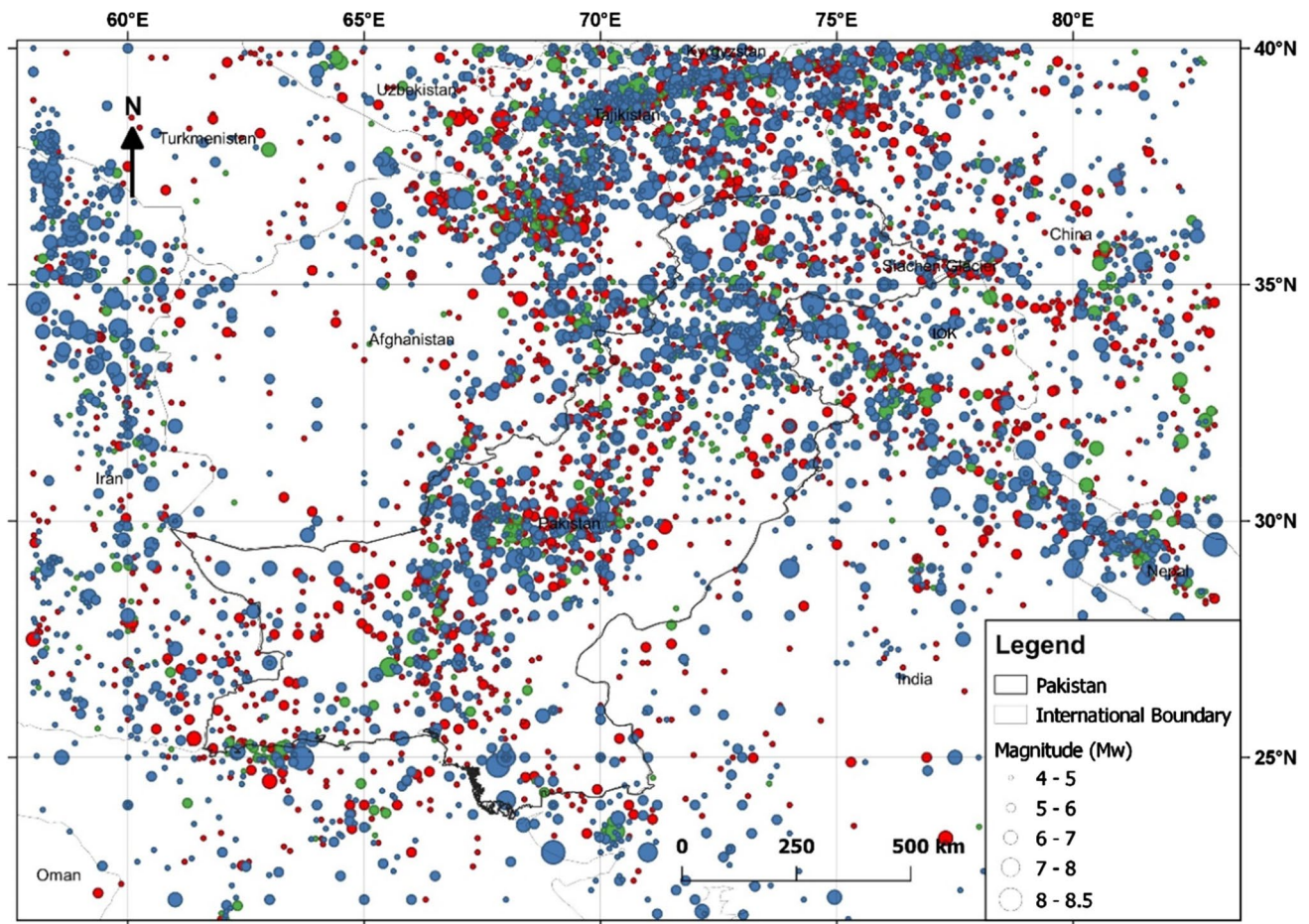


Fig. 6 Spatial distribution of shallow earthquakes (depth < 50 km); blue: 0–15 km depth, green: 15–30 km depth, red: 30–50 km depth

Department and Norwegian Seismic Array [50] has concluded similarly. The report presented the variation in past seismicity of Pakistan based on focal depths. Additionally, PMD & NOR-SAR (2007) reported that 80% of past seismicity is shallow (depth < 40 km) and only 20% of previous earthquake events have focal depths between 50 and 320 km.

Makran subduction zone shows intermediate to low seismicity except a few large earthquakes. The 1945 earthquake (M_w 8.2) is the maximum earthquake observed in this region. In this region, the Arabian plate is subducting under the Eurasian plate with a dip angle of 10 degrees extending 400–500 km towards the north [51]. The figure shows most of the events are having depths ranging between 5 and 55 km (Fig. 8).

3 Development of Updated Seismic Source Model

The development of a reliable seismic source model is a primary and important step for any seismic hazard assessment study [52]. The source model comprises of delineated area source zones and characterization of other seismogenic sources like faults and background seismicity. Based on the updated earthquake catalogue, two seismic source models (area source and spatially smoothed background seismicity) are presented for the seismic hazard assessment studies in Pakistan.

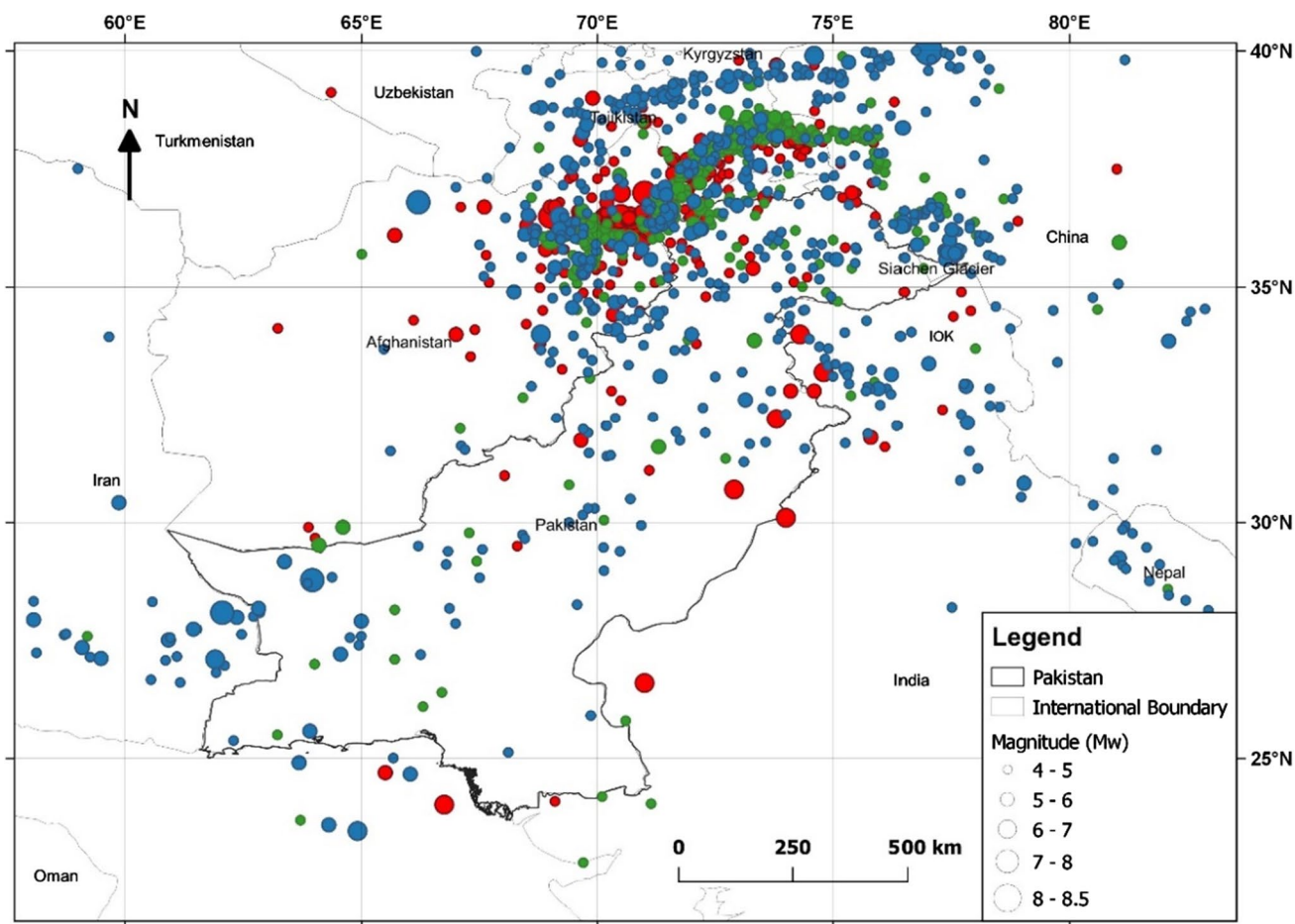


Fig. 7 Spatial distribution of intermediate-depth earthquakes ($50 \text{ km} < \text{depth} < 250 \text{ km}$); blue: 50–100 km depth, green: 100–150 km depth, red: 150–250 km depth

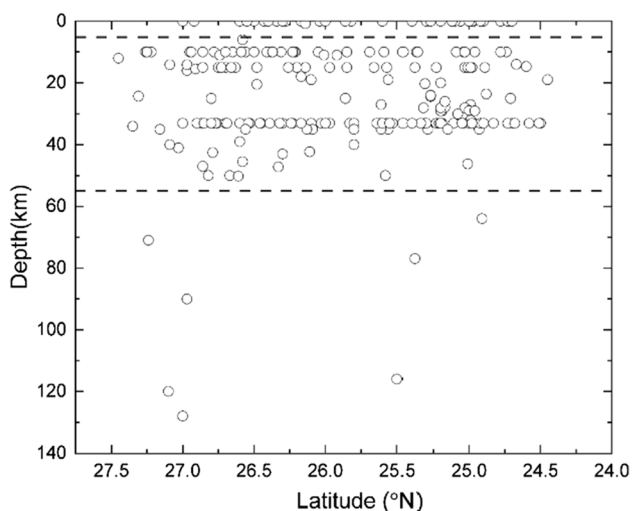


Fig. 8 Cross sections of the Makran subduction zone (MSZ) along longitude 57° E covering the historical events from 57° E to 66° E and latitude between 24° N and 27.5° N

3.1 Seismic Area Source Model

In probabilistic seismic hazard analysis, area sources are used for the representation of regions having homogenous seismicity. These area sources are often used for the modeling of seismicity pattern for those regions where the tectonic evidence are very rare. In the literature, various studies have delineated area sources for Pakistan that include Danciu et al. [53], Rafi et al. [31], Zhang et al. [54], Khan et al. [18], and NESPAK [19]. In this current study, Pakistan and the surrounding areas are divided into twenty-three (23) shallow crustal and five (5) deep source zones (Figs. 9 and 10). Small area sources are delineated and preferred over large source because the seismic hazard is reduced when large area sources are selected. This phenomenon is called spatial smearing [55]. The delineation of area sources is performed by considering the seismicity pattern, active crustal faults of the region, and principles of the Global Seismic Hazard Assessment Program [56] and Earthquake Model Middle East [53]. The area sources proposed by the

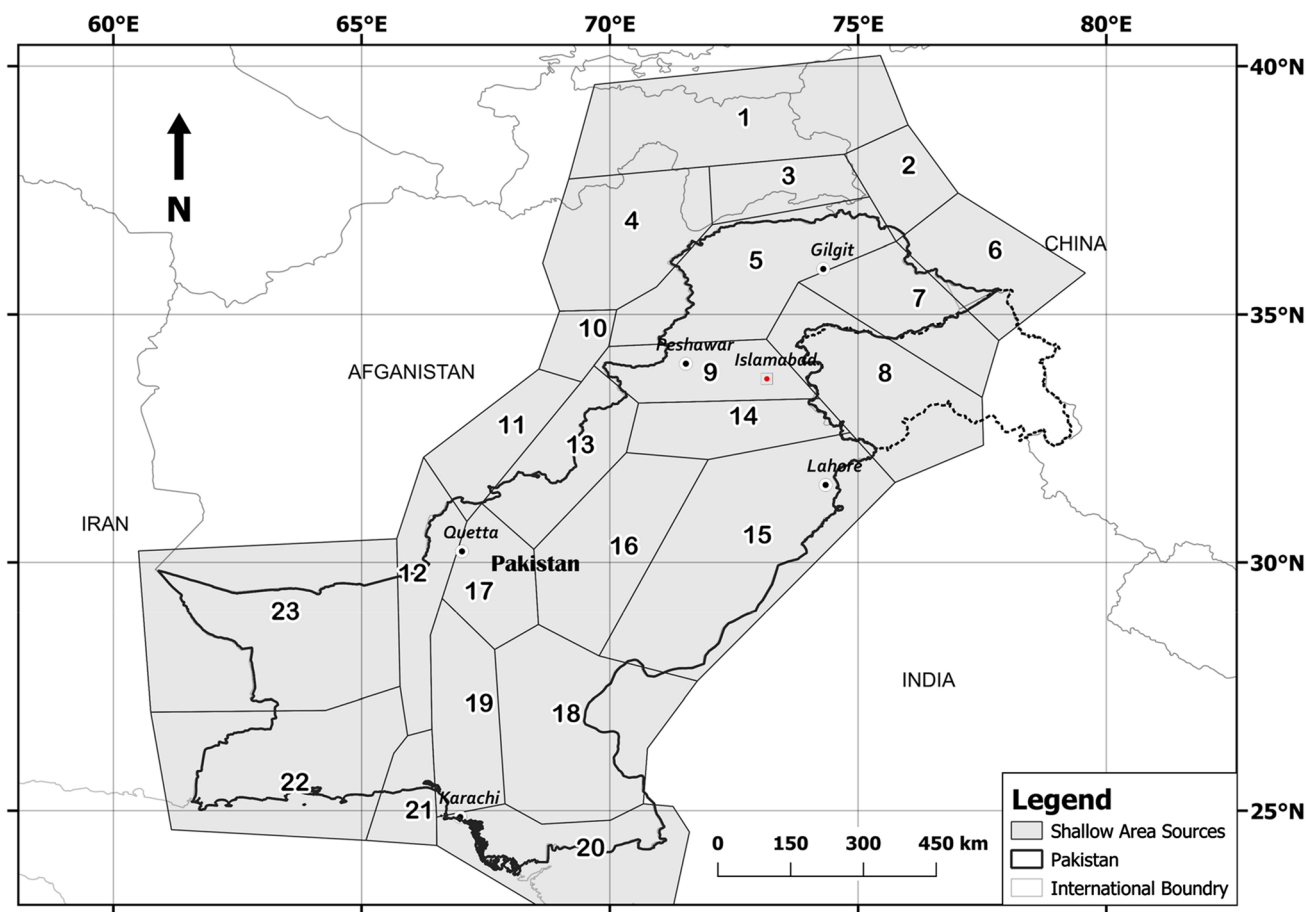


Fig. 9 The shallow seismic source zones divided based on active crustal faults and historical seismicity of that region

above-mentioned researchers were digitized/reproduced and combined to get an insight of the area sources of the past studies. In addition to this, the area sources in this current study are based on more updated catalogue which has higher number of earthquake events. The magnitude completeness periods for different magnitude ranges are greater than the previous studies. Number of area sources are comparatively higher as shown in Table 8. Furthermore, the seismo-tectonic of the region is accurately and precisely studied and taken into consideration while delineating area sources. These are the reasons which make this study more peculiar than the previous ones.

The recurrence rates for shallow and deep area sources are calculated by using the maximum likelihood method [57] and Gutenberg, Richter [44] magnitude distribution formula.

$$\text{Log } \lambda_M = a - b * M \quad (6)$$

where λ_M is the rate of earthquakes with magnitudes greater than and equal to moment magnitude (M), ' a ' is the y-intercept and ' b ' is negative slope of the exponential curve as shown in Figs. 11 and 12. The ' a ' value indicates the

overall rate of earthquakes in a region and ' b ' value indicates the relative ratio of small and large magnitudes [18]. It is assumed that the earthquake events with magnitude lower than $M_w 4$ may not result in any significant damage to the structures. Therefore, $M_w 4$ is selected as the lower bound magnitude (M_w^{min}). On the other hand, the maximum magnitude (M_w^{max}) in each area source is selected as the maximum observed magnitude plus 0.5. This margin of 0.5 is selected to account for any uncertainty in M_w^{max} estimation.

The seismicity parameters are extracted from the graphs which are plotted by using the updated version of the ZMAP tool [39]. The values of ' a ' and ' b ' for shallow and deep seismic sources were calculated and are shown in Tables 9 and 10, respectively. The seismogenic depth (D_{seis}) for all seismic sources is also determined and is presented along with other parameters. In shallow seismic sources, the variation in ' b ' value is from 0.529 to 1.23, while in deep seismic sources, the value ' b ' varies from 0.63 to 1.05. This variation in ' b ' is indicating that several major earthquakes ($M_w > 7$) have focal depths less than 50 km. The value of ' b ' is much lower for area sources located in the Hindukush region. The graph is being flattened due to several large earthquakes in



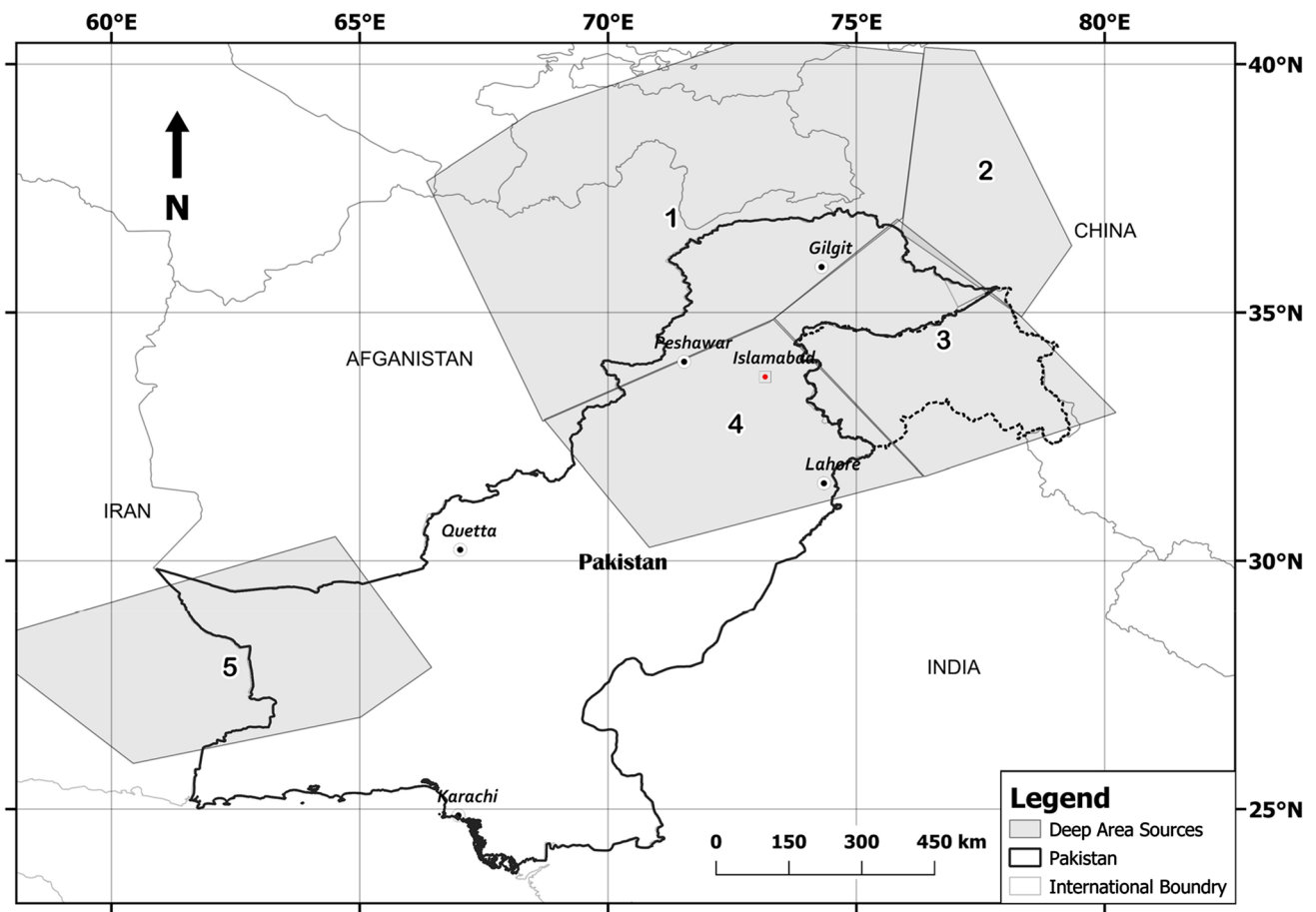


Fig. 10 The deep source zones delineated to count for the intermediate-depth earthquakes (<50 km depth <250 km)

Table 8 Comparison of various studies to the current study

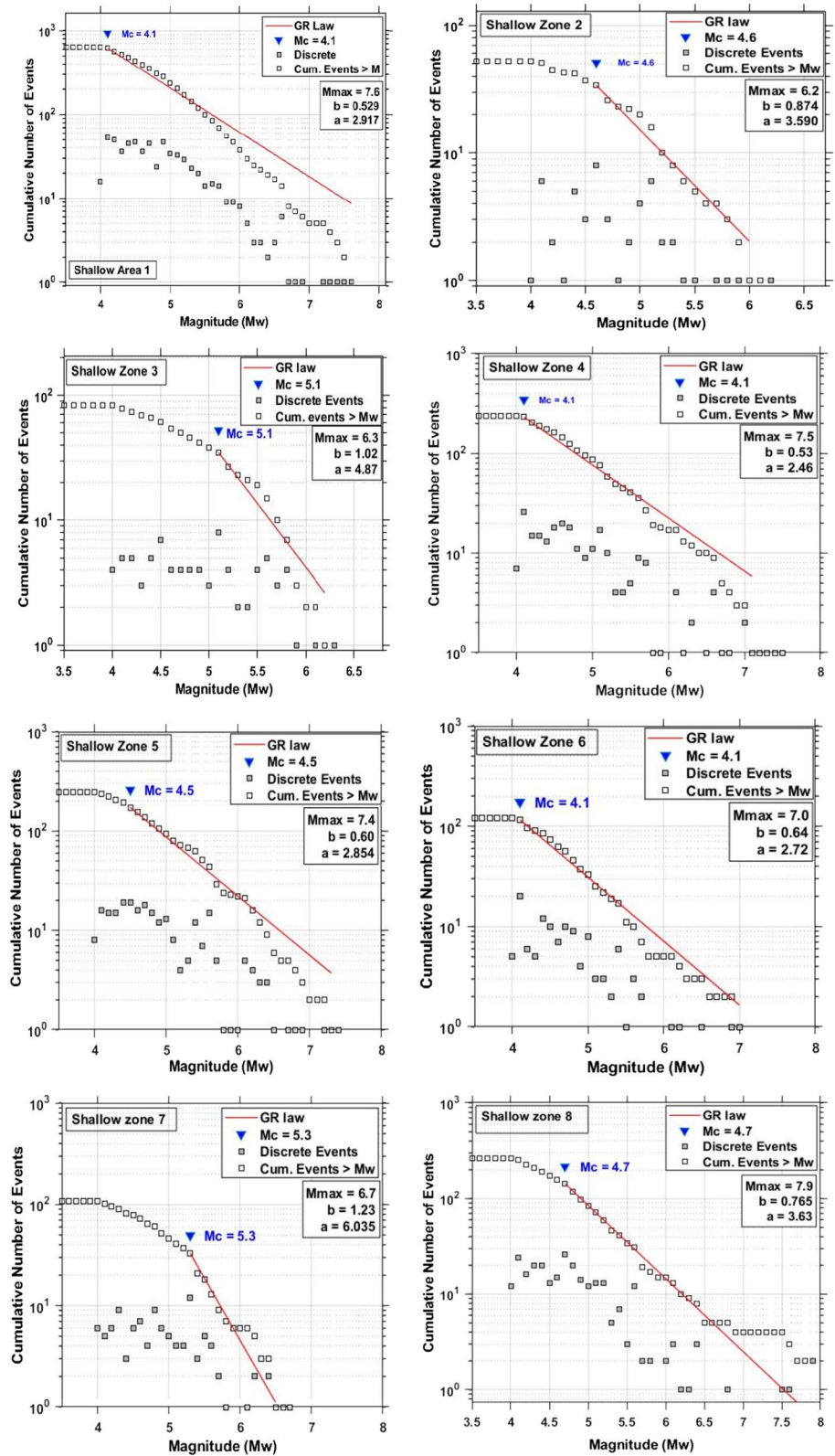
Parameters	Danciu et al. [53]	Rafi et al. [31]	Zhang et al. [54]	Khan et al. [18]	NESPAK [19]	Current study
No. of shallow area sources	18	16	19	20	17	23
No. of deep area sources	2	3	0	5	0	5

this region. The final catalogue has 112 earthquake events that are considered as major earthquakes ($M_w > 7$). 79% of those earthquakes have focal depths less than or equal to 50 km, while the remaining 21% were intermediate-depth earthquakes. Similarly, the value of λ_M in shallow seismic source varies from 0.36 to 13.18, while it varies from 0.68 to 40.08 in deep zones. The shallow zone 21 showed a minimum value of λ_M , i.e. 0.36 indicating least active seismic region having 23 number of events while the deep zone 5 depicted the maximum value of λ_M , i.e. 40.08 among all the seismic sources indicating the most active zone of the region. This seismic source has a 'b' value of 0.93 and a maximum moment magnitude of 7.5.

3.2 Spatially Smoothed Seismicity Model

A recent trend in the seismic hazard analysis is to explicitly model the crustal faults along with the background seismicity of the region. For this purpose, generally, the earthquake events are divided into two categories for the modelling of crustal faults and background seismicity. In such studies, the use of area source model alone is not considered sufficient to accurately predict the seismic hazard of an area. Therefore, besides the explicit modelling of faults, the background seismicity is also modelled as a spatially smoothed gridded seismicity model. Currently, such seismicity models are mostly being used in the probabilistic seismic hazard assessment studies [20,

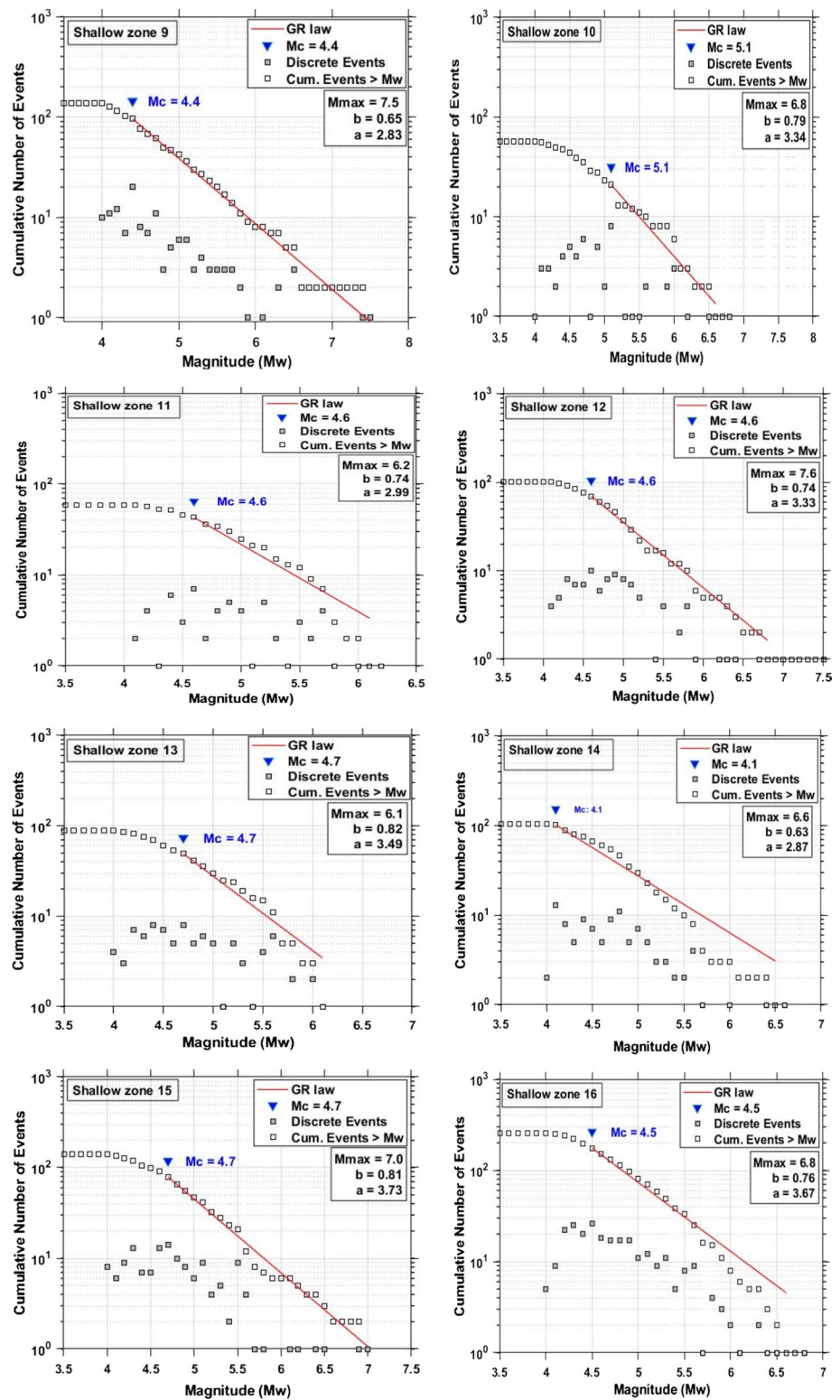
Fig. 11 Magnitude frequency distribution (MFD) curve for shallow seismic sources. The maximum likelihood method of Aki [57] is employed for obtaining seismicity parameters, i.e. a and b values



53, 58–60]. These studies assume that future earthquakes will occur near the small and moderate size events [60]. Ideally, the earthquake record for a thousand years is

required to predict the future hazard of a region. However, the available seismic data of the recorded earthquakes are too short to be relied upon for the spatio-temporal pattern

Fig. 11 (continued)



of future earthquakes. Due to the unavailability of data, the pattern of available past seismicity can be used as the predictor of the earthquake occurrence in the intra-plate region [61]. In the current study, spatially smoothed gridded seismicity rates have been calculated by using the

compiled earthquake catalogue. The smoothed activity rate, i.e. 10⁶ values are representing the earthquakes in mapped and unmapped fault areas as shown in Figs. 13 and 14. Besides dividing the region into small area zones, the region bounded by latitude 20°–40° N and longitude

Fig. 11 (continued)

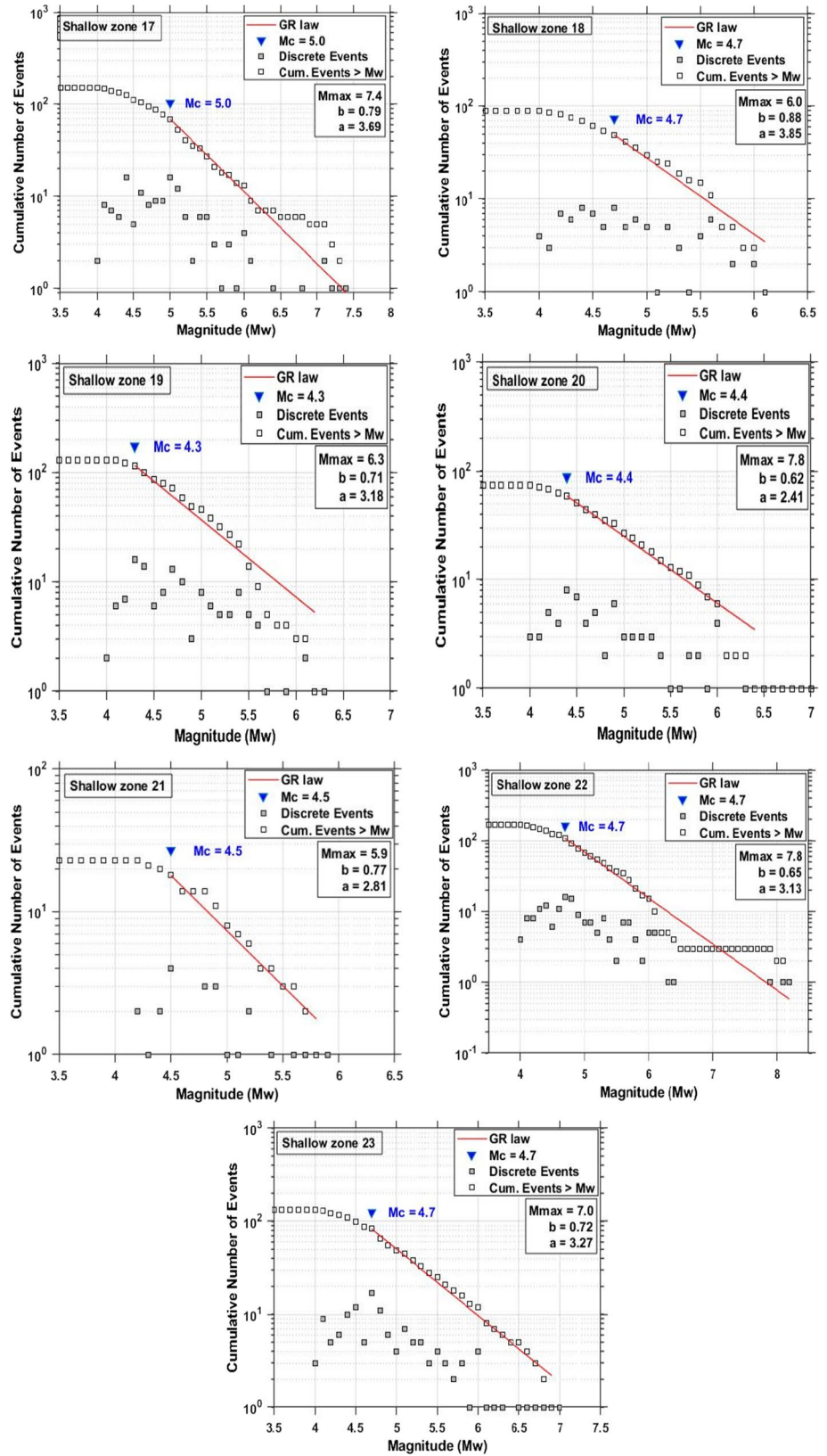
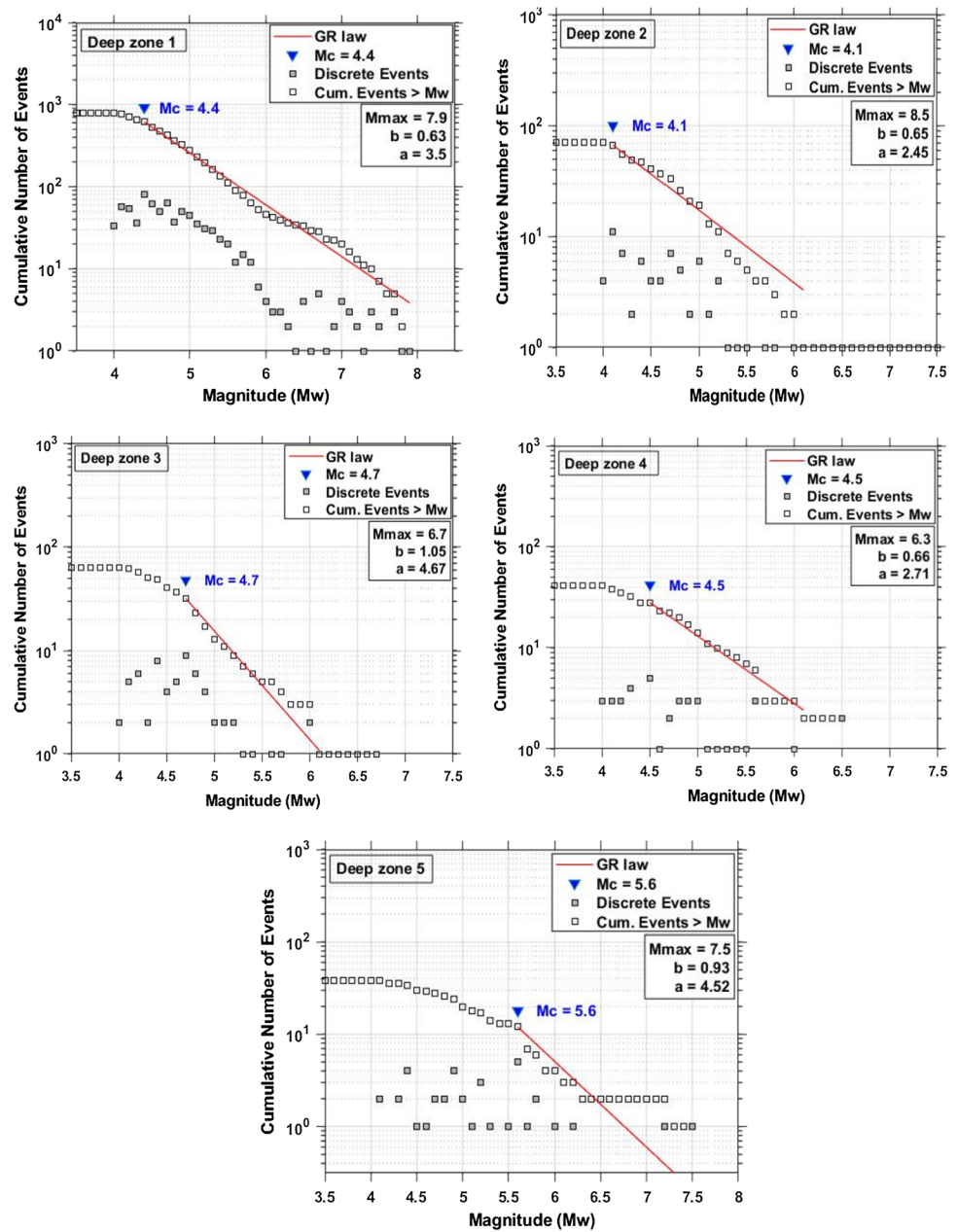


Fig. 12 Magnitude frequency distribution (MFD) curve for deep seismic sources. The maximum likelihood method of Aki [57] is employed for obtaining seismicity parameters, i.e. a and b values



58°–83° E is considered as a single large seismic source zone. The earthquake events reported in the region are divided into two layers based on their depths ranging from 0 to 50 km and 50 to 250 km. The region is divided into a grid of 0.1° in latitude and 0.1° in longitude. The variable catalogue completeness is taken into account by using the maximum likelihood method [62] for both shallow- and intermediate-depth seismicity for every grid cell. In this method, the earthquake’s data are classified into sets of magnitude ranges. The completion period is measured for each magnitude range to count the number of events for every range. Similarly, the seismicity rates are determined by counting the number of events having a magnitude

greater than the threshold value ($M_w = 4$) in each grid cell. The number of events represents the estimate of maximum likelihood 10^a value for each cell. The resulting 10^a values are the Gutenberg, Richter [44] annual rate of occurrence of each cell.

One constant value of ‘ b ’ is required to be used for spatial smoothed seismicity model which should be calculated by considering the whole study region as one seismic source [59]. The same methodology was adopted for this current study. Consequently, a uniform value of $b = 0.9$ is used, which was calculated from the magnitude-frequency distribution of complete and declustered earthquake catalogue. The seismicity rates are spatially smoothed using

Table 9 Seismicity parameters for 23 shallow area sources using the maximum likelihood method (Aki 1965)

Seismic zones	Events	<i>a</i>	<i>b</i>	M_C	D_{seis}	D_{max}	$M_{w_{min}}$	$M_{w_{max}}$	λ_M
1	637	2.917	0.529	4.1	33	50	4	7.6	6.37
2	52	3.590	0.874	4.6	33	37	4	6.2	1.24
3	83	4.87	1.02	5.1	33	43	4	6.3	6.17
4	239	2.46	0.53	4.1	32	50	4	7.5	2.13
5	246	2.854	0.60	4.5	32	50	4	7.4	2.92
6	121	2.72	0.64	4.1	33	49	4	7.0	1.47
7	107	6.035	1.23	5.3	32	50	4	6.7	13.18
8	264	3.63	0.765	4.7	32	50	4	7.9	3.72
9	136	2.83	0.65	4.4	34	48.4	4	7.5	1.69
10	57	3.34	0.79	5.1	33	50	4	6.8	1.42
11	59	2.99	0.74	4.6	33	43	4.1	6.2	0.90
12	101	3.33	0.741	4.6	32	50	4.1	7.6	1.96
13	89	3.49	0.82	4.7	33	47.2	4	6.1	1.58
14	104	2.87	0.63	4.1	32	50	4	6.6	2.16
15	142	3.73	0.81	4.7	32	50	4	7.0	2.98
16	257	3.67	0.76	4.5	33	50	4	6.8	4.43
17	150	3.69	0.79	5.0	33	43	4	7.4	3.55
18	70	3.85	0.88	4.7	33	50	4	6.0	2.14
19	131	3.18	0.71	4.3	34	38.5	4	6.3	2.25
20	74	2.42	0.62	4.4	33	48	4	7.8	0.91
21	23	2.81	0.77	4.5	32	44.8	4.2	5.9	0.36
22	74	3.13	0.65	4.7	33	48	4	7.8	3.42
23	133	3.27	0.72	4.7	33	50	4	7.0	2.52

Table 10 Seismicity parameters for five deep area sources using the maximum likelihood method [57]

Seismic zones	Number of events	<i>a</i>	<i>b</i>	M_C	D_{seis}	D_{max}	$M_{w_{min}}$	$M_{w_{max}}$	λ_M
1	795	3.5	0.63	4.4	55	456	4	7.9	9.55
2	71	2.45	0.65	4.1	65	311	4	8.5	0.68
3	64	4.67	1.05	4.7	56	750.6	4	6.7	3.09
4	41	2.71	0.66	4.5	60	372	4	6.3	1.13
5	38	5.42	0.93	5.6	55	185.9	4.1	7.5	40.08

λ is calculated using the $\log(\lambda) = a - b \times M_{w_{min}}$ relationship of Gutenberg, Richter [44]

the two-dimensional Gaussian function with a bandwidth of 50 km [58]. The bandwidth value is selected based on the catalogue location uncertainty and personal judgement.

4 Conclusions

An updated earthquake catalogue is compiled for Pakistan and surrounding areas bounded by coordinates latitude 20°–40° N and longitude 58°–83° E. It provides a comprehensive seismic data available for the seismic hazard assessment of the region. This catalogue is compiled by combining all the historical, pre-instrumental, and instrumentally recorded events from the available literature and online sources. The empirical expressions for the conversion of

data from other magnitude scales to the moment magnitude scale are developed for homogenizing all the events. For removing aftershocks and foreshocks, the declustering of this catalogue is performed by a computer package ZMAP [39]. The total number of events that remained after declustering is 7845 (AD10 – 2018CE). Using this catalogue, several shallow and deep seismic area sources are also delineated based on the seismicity pattern, seismotectonic, and faulting mechanism. The declustered catalogue is further processed for each seismic source zone to compute seismic parameters (i.e. ‘*a*’ and ‘*b*’ value). The catalogue contains six events with $M_w > 8$, while 93 events are between M_w 7 and M_w 8. The completeness analysis is performed using the visual cumulative method [41] and [42] method. For this purpose, the OpenQuake engine [45] is used. The magnitude



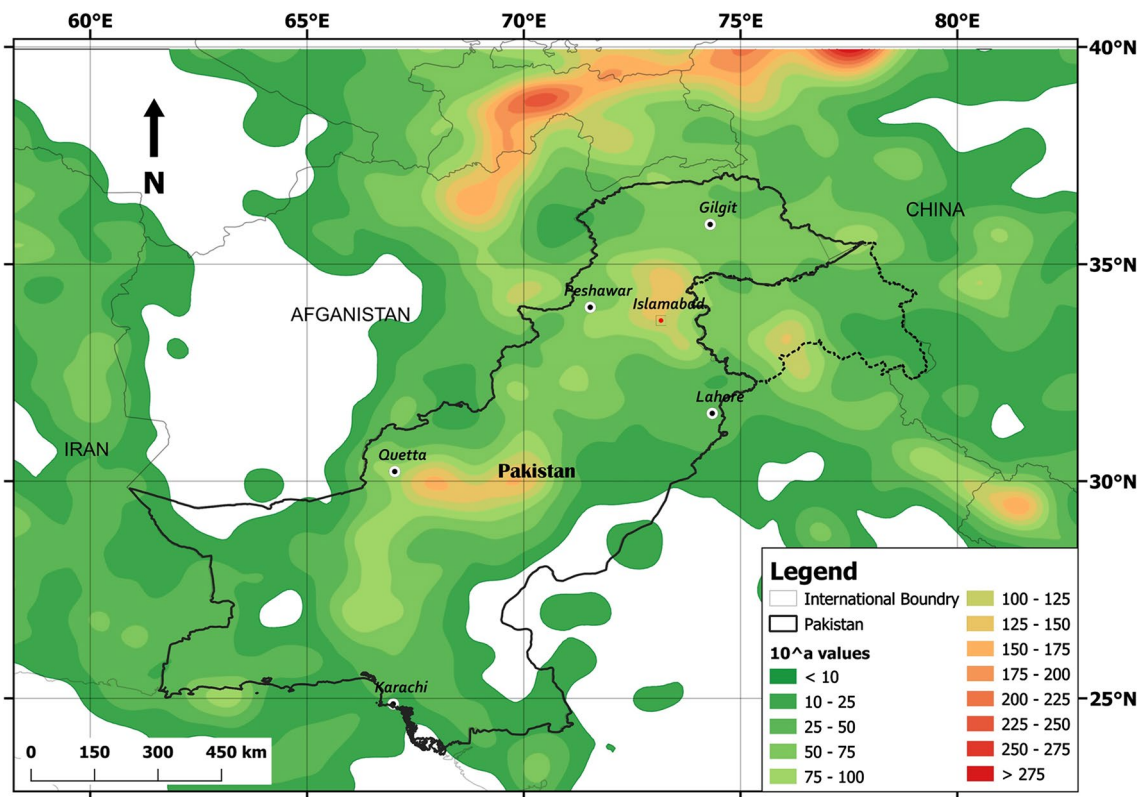


Fig. 13 Smoothed activity rate 10^a the value derived for seismicity from 0–50 km depth

of completeness is determined using the Gutenberg, Richter [44] magnitude-frequency distribution method for all seismic sources. Finally, using the developed catalogue, the smoothed activity rates for spatially smoothed gridded seismicity model are also determined for two layers of depths (from 0 to 50 km and 50 to 250 km). The developed catalogue, seismic source models, and recurrence parameters can be effectively used in the probabilistic seismic hazard analysis (PSHA) of Pakistan and its surroundings.

Appendix: Data Sources

The data sources used for the compilation of earthquake catalogue comprises of the available literature, international databases, and local databases. Information about these sources are available online, but a brief introduction of these sources is presented here.

International Sources

- (a) International Seismological Centre (ISC)
The ISC <http://www.isc.ac.uk/iscbulletin/search/catalogue/> is established in 1964, carrying the work

of its predecessor International Seismological Summary (ISS). The ISS published its first bulletin in 1918. ISC is the international archive for reliable earthquake events. It contains all the data from PDE and hundreds of other regional and local sources. The reviewed earthquake’s origin by ISC is considered most reliable [33]. About 10,000 events on average are reviewed per month, in which approximately 40% events are manually reviewed.

- (b) Preliminary Determination of Epicenters (PDE)
PDE is the archival of the USGS earthquake catalogue. It contains the origin, magnitude, and arrival time of earthquake events located by the National Earthquake Information Centre (NEIC) and other contributing U.S national and foreign sources. In 1940, NEIC produced its first monthly publication, which was called the Preliminary Determination of Epicenter or PDE. The NEIC established in 1966 by the Environmental Science Services Administration (ESSA) is likely to report the origin, time, and size of earthquakes rapidly worldwide.
- (c) Global Centroid Moment Tensor (GCMT)
The project was started by Adam Dziewonski at Harvard University by the name Harvard CMT project from 1982 to 2006. After 2006, the research moves forward

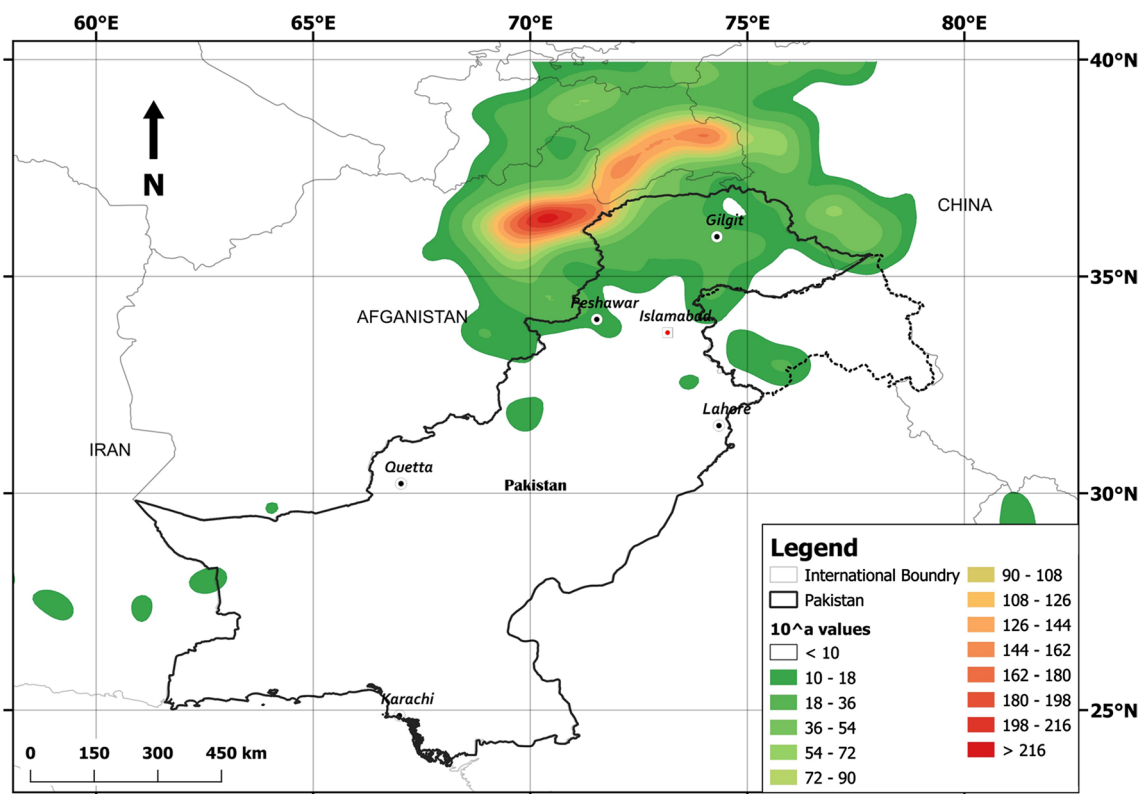


Fig. 14 Smoothed activity rate 10^a the value derived for seismicity from 50 – 250 km depth

under the name “The Global Centroid Moment Tensor.” The project has the aim to calculate CMT solutions for events having magnitude greater than $M_w = 5.5$. The catalogue of GCMT can be accessed online at <http://www.globalcmt.org>.

Local Sources

In Pakistan, the local seismic station’s network started working back in 1954 with the installation of World Wide Standard Seismographic Network (WWSSN) by United States Geological Survey (USGS). In 1975, the Micro Seismic Study Program (MSSP) under the Pakistan Atomic Energy Commission (PAEC) installed a seismic stations network. This network comprises of 30 seismic stations all over Pakistan. After the devastating 2005 Kashmir earthquake, the Pakistan Metrological Department (PMD) decided to expand its seismic station’s network by installing the broadband sensors and accelerometers.

(a) National Geophysical Data Centre (NGDC)

The National Geophysical Data Centre provides important historical earthquake events ranges in date from 2150 BCE to the present. The events are com-

plied from the previous literature, local and worldwide catalogues, and single event reports. Earthquake origin information of the recent historical events is obtained from the PDE. Local Sources.

(b) Pakistan Meteorological Department (PMD):

The Pakistan Meteorological Department (PMD) started recording earthquake events in 1974 in Pakistan and nearby areas. The PMD provides 58 events for the period of AD 25 – 1905 CE [63]. Many of those are extracted from the catalogue of [30]. PMD has installed twenty seismic monitoring stations all over the Pakistan and Azad Jammu & Kashmir. These stations contain broadband (120 s) sensors. PMD central recording stations are located at Karachi and Islamabad and connected through satellite communication system with all other stations. PMD has also started a programme for the installation of a short period (1 s) sensors for the close monitoring of fault and local seismicity. There is also a Global Seismographic Network (GSN) station located in Islamabad, Nilore. The Global Seismographic Network is a digital network of seismological and geophysical sensors, connected through a telecommunications network, used for monitoring, research, and education. GSN is developed by the partnership of the USGS, the National Science Foundation (NSF), and



the Incorporated Research Institutions for Seismology (IRIS). The GSN has 150 modern seismic stations all over the world. GSN data are stored in the IRIS Data Management Centre.

- (c) Water and Power Development Authority (WAPDA)
Water and Power Development Authority (WAPDA) established a seismic network of nine short periods, VHF radio telemetered stations in 1973 around Tarbela dam with the help of Lamont Doherty Geological Observatory of Columbia University, USA. Now, Wapda's seismic monitoring system consists of 29 online stations powered up by the solar system and connected to Tarbela data centre via the V-sat communication system. Ten online stations around the Tarbela dam project, six online stations around Dasu dam project, three online stations around Bunji dam project, and ten online stations around Basha dam.

References

- Kazmi, A.H.; Rana, R.: Tectonic map of Pakistan: Ministry of Petroleum and Natural Resources. In: Geological Survey of Pakistan (1982)
- Chen, Z.; Burchfiel, B.C.; Liu, Y.; King, R.W.; Royden, L.H.; Tang, W.; Wang, E.; Zhao, J.; Zhang, X.: Global positioning system measurements from eastern Tibet and their implications for India/Eurasia intercontinental deformation. *J. Geophys. Res. Atmos.* **105**(B7), 16215–16227 (2000). <https://doi.org/10.1029/2000jb900092>
- Khan, M.A.; Bendick, R.; Bhat, M.I.; Bilham, R.; Kakar, D.M.; Khan, S.F.; Lodi, S.H.; Qazi, M.S.; Singh, B.; Szeliga, W.: Preliminary geodetic constraints on plate boundary deformation on the western edge of the Indian plate from TriGGnet (Tri-University GPS geodesy network). *J. Himal. Earth Sci* **41**, 71–87 (2008)
- Molnar, P.; Tapponnier, P.: Relation of the tectonics of eastern China to the India–Eurasia collision: application of slip-line field theory to large-scale continental tectonics. *Geology* **5**(4), 212–216 (1977)
- Perry, M.; Kakar, N.; Ischuk, A.; Metzger, S.; Bendick, R.; Molnar, P.; Mohadjer, S.: Little geodetic evidence for localized Indian subduction in the Pamir-Hindu Kush of Central Asia. *Geophys. Res. Lett.* **46**(1), 109–118 (2019). <https://doi.org/10.1029/2018GL080065>
- Seeber, L.; Armbruster, J.G.; Quittmeyer, R.C.: Seismicity and continental subduction in the Himalayan arc. In: Gupta, H.K.; Delany, F.M. (Eds.) *Zagros Hindu Kush Himalaya Geodynamic Evolution*, Vol. 3, pp. 215–242. American Geophysical Union, Washington DC (1981)
- Khwaja, A.A.; Jan, M.Q.: The 8 October 2005 Muzaffarabad earthquake: Preliminary seismological investigations and probabilistic estimation of peak ground accelerations. *Curr. Sci. Bangalore*, 1158–1166 (2008)
- Negredo, A.M.; Replumaz, A.; Villaseñor, A.; Guillot, S.: Modeling the evolution of continental subduction processes in the Pamir-Hindu Kush region. *Earth Planet. Sci. Lett.* **259**(1–2), 212–225 (2007). <https://doi.org/10.1016/j.epsl.2007.04.043>
- Quittmeyer, R.C.; Farah, A.; Jacob, K.H.: The seismicity of Pakistan and its relation to surface faults. *Geodyn. Pak.* 271–284 (1979)
- Apel, E.T.; Bürgmann, R.; Banerjee, P.: Geodetically constraining Indian plate motion and implications for plate boundary deformation (2006)
- Farhoudi, G.; Karig, D.: Makran of Iran and Pakistan as an active arc system. *Geology* **5**(11), 664–668 (1977). [https://doi.org/10.1130/0091-7613\(1977\)5-664](https://doi.org/10.1130/0091-7613(1977)5-664)
- Shearman, D.; Walker, G.; Booth, B.; Falcon, N.: The geological evolution of southern Iran: the report of the Iranian Makran expedition. *Geogr. J.* **142**, 393–410 (1976). <https://doi.org/10.2307/1795293>
- Stoneley, R.: Evolution of the continental margins bounding a former southern Tethys. In: Burk, Creighton A.; Drake, Charles L. (Eds.) *The Geology of Continental Margins*, pp. 889–903. Springer, Berlin (1974)
- Zarifi, Z.; Raeesi, M.: Heterogeneous coupling along Makran subduction zone. In: AGU Fall Meeting Abstracts (2010)
- Fujiwara, S.; Tobita, M.; Sato, H.P.; Ozawa, S.; Une, H.; Koarai, M.; Nakai, H.; Fujiwara, M.; Yurai, H.; Nishimura, T.: Satellite data gives snapshot of the 2005 Pakistan earthquake. *Eos Trans. Am. Geophys. Union* **87**(7), 73–77 (2006). <https://doi.org/10.1029/2006EO070001>
- Kaneda, H.; Nakata, T.; Tsutsumi, H.; Kondo, H.; Sugito, N.; Awata, Y.; Akhtar, S.S.; Majid, A.; Khattak, W.; Awan, A.A.: Surface rupture of the 2005 Kashmir, Pakistan, earthquake and its active tectonic implications. *Bull. Seismol. Soc. Am.* **98**(2), 521–557 (2008). <https://doi.org/10.1785/0120070073>
- Durrani, A.J.; Elnashai, A.S.; Hashash, Y.M.A.; Kim, S.J.; Masud, A.: The Kashmir earthquake of October 08, 2005, p. 51 (2005)
- Khan, S.; Waseem, M.; Khan, M.A.; Ahmed, W.: Updated earthquake catalogue for seismic hazard analysis in Pakistan. *J. Seismolog.* **22**(4), 841–861 (2018). <https://doi.org/10.1007/s10950-018-9736-y>
- NESPAK: Building code of Pakistan—seismic hazard evaluation studies. In: Ministry of Housing and Works, Government of Pakistan (2007)
- Zare, M.; Amini, H.; Yazdi, P.; Sesetyan, K.; Demircioglu, M.B.; Kalafat, D.; Erdik, M.; Giardini, D.; Khan, M.A.; Tsereteli, N.: Recent developments of the Middle East catalog. *J. Seismolog.* **18**(4), 749–772 (2014). <https://doi.org/10.1007/s10950-014-9444-1>
- PBC: Building code of Pakistan, Seismic Provision-2007. In: Ministry of Housing and Works, Islamabad, Pakistan (2007)
- ISC: International Seismological Centre. On-line Bulletin (2019)
- USGS: USGS. <https://earthquake.usgs.gov/earthquakes/search/> (2019). Accessed 10 Apr 2019
- Council, N.R.: Review of NOAA's national geophysical data center. National Academies Press, Washington DC (2018)
- Dziewonski, A.; Chou, T.; Woodhouse, J.: Determination of earthquake source parameters from waveform data for studies of global and regional seismicity. *J. Geophys. Res. Solid Earth* (1981). <https://doi.org/10.1029/JB086iB04p02825>
- Ekström, G.; Nettles, M.; Dziewoński, A.: The global CMT project 2004–2010: centroid-moment tensors for 13,017 earthquakes. *Phys. Earth Planet. Inter.* **200**, 1–9 (2012). <https://doi.org/10.1016/j.pepi.2012.04.002>
- Ambraseys, N.: Reappraisal of north-Indian earthquakes at the turn of the 20th century. *Curr. Sci. Bangalore* **79**(9), 1237–1250 (2000)
- Ambraseys, N.; Bilham, R.: The tectonic setting of Bamiyan and seismicity in and near Afghanistan for the past twelve centuries. In: Margottini, Claudio (Ed.) *After the Destruction of*



- Giant Buddha Statues in Bamiyan (Afghanistan) in 2001, pp. 101–152. Springer, Berlin (2014)
29. Ambraseys, N.N.; Douglas, J.: Magnitude calibration of north Indian earthquakes. *Geophys. J. Int.* **159**(1), 165–206 (2004). <https://doi.org/10.1111/j.1365-246x.2004.02323.x>
 30. Quittmeyer, R.; Jacob, K.: Historical and modern seismicity of Pakistan, Afghanistan, northwestern India, and southeastern Iran. *Bull. Seismol. Soc. Am.* **69**(3), 773–823 (1979)
 31. Rafi, Z.; Lindholm, C.; Bungum, H.; Laghari, A.; Ahmed, N.: Probabilistic seismic hazard of Pakistan, Azad-Jammu Kashmir. *Nat Hazards* **61**(3), 1317–1354 (2012). <https://doi.org/10.1007/s11069-011-9984-4>
 32. Scordilis, E.: Empirical global relations converting M_S and mb to moment magnitude. *J. Seismolog.* **10**(2), 225–236 (2006). <https://doi.org/10.1007/s10950-006-9012-4>
 33. Yadav, R.; Bormann, P.; Rastogi, B.; Das, M.; Chopra, S.: A homogeneous and complete earthquake catalog for northeast India and the adjoining region. *Seismol. Res. Lett.* **80**(4), 609–627 (2009)
 34. Lolli, B.; Gasperini, P.; Vannucci, G.: Erratum: Empirical conversion between teleseismic magnitudes (mb and Ms) and moment magnitude (Mw) at the Global, Euro-Mediterranean and Italian scale. *Geophys. J. Int.* **200**(1), 199–199 (2014). <https://doi.org/10.1093/gji/ggu385>
 35. Akkar, S.; Çağnan, Z.; Yenier, E.; Erdoğan, Ö.; Sandikkaya, M.A.; Gülkan, P.: The recently compiled Turkish strong motion database: preliminary investigation for seismological parameters. *J. Seismolog.* **14**(3), 457–479 (2010). <https://doi.org/10.1007/s10950-009-9176-9>
 36. Gardner, J.; Knopoff, L.: Is the sequence of earthquakes in Southern California, with aftershocks removed, Poissonian? *Bull. Seismol. Soc. Am.* **64**(5), 1363–1367 (1974)
 37. Reasenber, P.: Second-order moment of central California seismicity, 1969–1982. *J. Geophys. Res.* **90**(B7), 5479–5495 (1985). <https://doi.org/10.1029/JB090iB07p05479>
 38. Uhrhammer, R.: Characteristics of northern and central California seismicity. *Earthq. Notes* **57**(1), 21 (1986)
 39. Wiemer, S.: A software package to analyze seismicity: ZMAP. *Seismol. Res. Lett.* **72**(3), 373–382 (2001). <https://doi.org/10.1785/gssrl.72.3.373>
 40. Rydelek, P.A.; Sacks, I.S.: Testing the completeness of earthquake catalogues and the hypothesis of self-similarity. *Nature* **337**(6204), 251 (1989)
 41. Tinti, S.; Mulargia, F.: Completeness analysis of a seismic catalog. *Ann. Geophys.* **3**, 407–414 (1985)
 42. Stepp, J.: Analysis of completeness of the earthquake sample in the Puget Sound area. In: NOAA Tech. Report ERL 267-ESL30, Boulder, Colorado (1973)
 43. Woessner, J.; Wiemer, S.: Assessing the quality of earthquake catalogues: estimating the magnitude of completeness and its uncertainty. *Bull. Seismol. Soc. Am.* **95**(2), 684–698 (2005)
 44. Gutenberg, B.; Richter, C.F.: Frequency of earthquakes in California. *Bull. Seismol. Soc. Am.* **34**(4), 185–188 (1944)
 45. Pagani, M.; Monelli, D.; Weatherill, G.; Danciu, L.; Crowley, H.; Silva, V.; Henshaw, P.; Butler, L.; Nastasi, M.; Panzeri, L.: OpenQuake engine: an open hazard (and risk) software for the global earthquake model. *Seismol. Res. Lett.* **85**(3), 692–702 (2014). <https://doi.org/10.1785/0220130087>
 46. Tichelaar, B.W.; Ruff, L.J.: Depth of seismic coupling along subduction zones. *J. Geophys. Res. Solid Earth.* **98**(B2), 2017–2037 (1993). <https://doi.org/10.1029/92jb02045>
 47. Scholz, C.H.: *The mechanics of earthquakes and faulting*. Cambridge university press, (2019)
 48. Maggi, A.; Priestley, K.; Jackson, J.: Focal depths of moderate and large size earthquakes in Iran. *J. Seismolog.* **4**(2–3), 1–10 (2002)
 49. Yano, T.E.; Takeda, T.; Matsubara, M.; Shiomi, K.: Japan unified high-resolution relocated catalog for earthquakes (JUICE): crustal seismicity beneath the Japanese Islands. *Tectonophysics* **702**, 19–28 (2017). <https://doi.org/10.1016/j.tecto.2017.02.017>
 50. PMD, NORSAR: Seismic hazard analysis and zonation of Pakistan, Azad Jammu and Kashmir. Pakistan Meteorological Department (2007)
 51. Byrne, D.E.; Sykes, L.R.; Davis, D.M.: Great thrust earthquakes and aseismic slip along the plate boundary of the Makran subduction zone. *J. Geophys. Res. Solid Earth* **97**(B1), 449–478 (1992). <https://doi.org/10.1029/91jb02165>
 52. El-Hussain, I.; Al-Shijbi, Y.; Deif, A.; Mohamed, A.; Ezzelarab, M.: Developing a seismic source model for the Arabian Plate. *Arab. J. Geosci.* **11**(15), 435 (2018)
 53. Danciu, L.; Şeşetyan, K.; Demircioglu, M.; Gülen, L.; Zare, M.; Basili, R.; Elias, A.; Adamia, S.; Tsereteli, N.; Yalçın, H.; Utkucu, M.; Khan, M.A.; Sayab, M.; Hessami, K.; Rovida, A.N.; Stucchi, M.; Burg, J.-P.; Karakhanian, A.; Babayan, H.; Avanesyan, M.; Mammadli, T.; Al-Qaryouti, M.; Kalafat, D.; Varazanashvili, O.; Erdik, M.; Giardini, D.: The 2014 earthquake model of the Middle East: seismogenic sources. *Bull. Earthq. Eng.* **16**(8), 3465–3496 (2018). <https://doi.org/10.1007/s10518-017-0096-8>
 54. Zhang, P.; Yang, Z.; Gupta, H.K.; Bhatia, S.C.; Shedlock, K.M.: Global seismic hazard assessment program (GSHAP) in continental Asia (1999)
 55. Aki, K.: Probabilistic seismic hazard analysis. National Academies, (1988)
 56. Giardini, D.; Grünthal, G.; Shedlock, K.M.; Zhang, P.: The GSHAP global seismic hazard map. *Ann. Geophys.* **42**(6) (1999)
 57. Aki, K.: Maximum likelihood estimate of b in the formula $\log N = a - bM$ and its confidence limits. *Bull. Earthq. Res. Inst. Tokyo Univ.* **43**, 237–239 (1965)
 58. Frankel, A.: Mapping seismic hazard in the central and eastern United States. *Seismol. Res. Lett.* **66**(4), 8–21 (1995). <https://doi.org/10.1785/gssrl.66.4.8>
 59. Ornthammarath, T.; Warnitchai, P.; Worakanchana, K.; Zaman, S.; Sigbjörnsson, R.; Lai, C.G.: Probabilistic seismic hazard assessment for Thailand. *Bull. Earthq. Eng.* **9**(2), 367–394 (2011). <https://doi.org/10.1007/s10518-010-9197-3>
 60. Petersen, M.D.; Moschetti, M.P.; Powers, P.M.; Mueller, C.S.; Haller, K.M.; Frankel, A.D.; Zeng, Y.; Rezaeian, S.; Harmsen, S.C.; Boyd, O.S.: The 2014 United States national seismic hazard model. *Earthq. Spectra* **31**(S1), S1–S30 (2015)
 61. Stein, S.; Geller, R.J.; Liu, M.: Why earthquake hazard maps often fail and what to do about it. *Tectonophysics* **562**, 1–25 (2012). <https://doi.org/10.1016/j.tecto.2012.06.047>
 62. Weichert, D.H.: Estimation of the earthquake recurrence parameters for unequal observation periods for different magnitudes. *Bull. Seismol. Soc. Am.* **70**(4), 1337–1346 (1980)
 63. Ali, M.: *Seismic Hazard Analysis of Pakistan*. Pakistan Institute of Engineering & Applied Sciences, Nilore, Islamabad, Pakistan (2011)
 64. Bird, P.: An updated digital model of plate boundaries. *Geophys. Geosyst. Geochem.* (2003). <https://doi.org/10.1029/2001gc000252>
 65. Jade, S.: Estimates of plate velocity and crustal deformation in the Indian subcontinent using GPS geodesy. *Current Science-Bangalore* 1443–1448 (2004)
 66. Sella, G.F.; Dixon, T.H.; Mao, A.: REVEL: a model for recent plate velocities from space geodesy. *J. Geophys. Res.* **107**(B4), ETG11-1-ETG11-30 (2002). <https://doi.org/10.1029/2000jg000033>
 67. Vernant, P.; Nilforoushan, F.; Hatzfeld, D.; Abbassi, M.R.; Vigny, C.; Masson, F.; Nankali, H.; Martinod, J.; Ashtiani, A.;



- Bayer, R.; Tavakoli, F.; Chéry, J.: Present-day crustal deformation and plate kinematics in the Middle East constrained by GPS measurements in Iran and northern Oman. *Geophys. J. Int.* **157**(1), 381–398 (2004). <https://doi.org/10.1111/j.1365-246X.2004.02222.x>JGeophysicalJournalInternational
68. van Stiphout, T.; Zhuang, J.; Marsan, D.: Seismicity declustering. *Community Online Resource for Statistical Seismicity Analysis* **10**(1) (2012)

